Identification of 4-(4-nitro-2-phenethoxyphenyl)pyridine as a promising new lead for discovering inhibitors of both human and rat 11β-Hydroxylase

ARTICLE *in* EUROPEAN JOURNAL OF MEDICINAL CHEMISTRY · MAY 2015

Impact Factor: 3.45 · DOI: 10.1016/j.ejmech.2015.04.013

4 AUTHORS, INCLUDING:

Qingzhong Hu

University of Cambridge

Nina Hanke

Universität des Saarlandes

European Journal of Medicinal Chemistry 96 (2015) 139–150

Contents lists available at ScienceDirect

European Journal of Medicinal Chemistry

journal homepage: http://www.elsevier.com/locate/ejmech

Original article

Identification of 4-(4-nitro-2-phenethoxyphenyl)pyridine as a promising new lead for discovering inhibitors of both human and rat 11β-Hydroxylase

Qingzhong Hu [a, b], Jessica Kunde [a], Nina Hanke [c], Rolf W. Hartmann [a, b, *]

[a] Pharmaceutical and Medicinal Chemistry, Saarland University, Campus C2.3, D-66123 Saarbrücken, Germany
[b] Helmholtz Institute for Pharmaceutical Research Saarland (HIPS), Campus C2.3, D-66123 Saarbrücken, Germany
[c] Elexopharm GmbH, Campus A1, 66123 Saarbrücken, Germany

A R T I C L E   I N F O

Article history:
Received 28 January 2015
Received in revised form
3 April 2015
Accepted 6 April 2015
Available online 8 April 2015

Keywords:
11*β*-hydroxylase
Human and rat CYP11B1
Inhibitors
Cushing's syndrome
Selectivity
Aromatase

A B S T R A C T

The inhibition of 11*β*-hydroxylase is a promising strategy for the treatment of Cushing's syndrome, in particular for the recurrent and subclinical cases. To achieve proof of concept in rats, efforts were paid to identify novel lead compounds inhibiting both human and rat CYP11B1. Modifications on a potent promiscuous inhibitor of *h*CYP11B1, *h*CYP11B2 and *h*CYP19 (compound **IV**) that exhibited moderate *r*CYP11B1 inhibition led to compound **8** as a new promising lead compound. Significant improvements compared to starting point **IV** were achieved regarding inhibitory potency against both human and rat CYP11B1 (IC_{50} values of 2 and 163 nM, respectively) as well as selectivity over *h*CYP19 (IC_{50} = 1900 nM). Accordingly, compound **8** was around 7- and 28-fold more potent than metyrapone regarding the inhibition of human and rat CYP11B1 and exhibited a comparable selectivity over *h*CYP11B2 (SF of 3.5 vs 4.9). With further optimizations on this new lead compound **8**, drug candidates with satisfying profiles are expected to be discovered.

1. Introduction

Although endogenous Cushing's syndrome is a rare disease with an annual incidence as low as 2–3 cases per million of the population [1], it leads to a high mortality via co-morbidities including cardio- and cerebrovascular diseases [1,2]. As for the majority of this syndrome that are caused by pituitary adenomas and termed Cushing's disease, the 5 years' survival is only about 50% if without effective treatments [3]. Despite of the fact that the surgical removal of tumors leads to cure or remission in 65–85% of patients, recurrences are observed in up to 20% of cases [1]. Furthermore, investigations indicate a high prevalence of undiagnosed subclinical Cushing's syndrome in particular in patients with type II diabetes and osteoporosis [4,5]. Although no evident symptoms other than high levels of cortisol in plasma are observed in these patients, this syndrome is considered to exacerbate concomitant diseases. More severe is that subclinical Cushing's syndrome is deemed to be associated with metabolic dementia and to promote the progression of Alzheimer disease [6]. Apparently, for these recurrent and subclinical cases, pharmacotherapy via the inhibition of steroid 11*β*-hydroxylase (*h*CYP11B1), which catalyzes the hydroxylation of 11-deoxycortisol to cortisol, to reduce the circulating cortisol levels is a superior approach. Metyrapone (IC_{50} = 15 nM, Chart 1) as an inhibitor of adrenal steroidogenesis has been employed to relieve patients' symptoms before surgery [7]; and its long-term applications were also reported to successfully control cortisol levels and psychiatric manifestations [8,9]. In a phase I clinical study, an experimental *h*CYP11B1 inhibitor LCI699 (IC_{50} = 2.9 nM, Chart 1) normalized urinary free cortisol levels or reduced its concentrations by more than half from baseline in patients with moderate-to-severe Cushing's disease [10]. However, simultaneously, the plasma aldosterone levels were significantly decreased by around 3-fold from 4.2 to 1.3 ng/dL because of the potent inhibition of aldosterone synthase (*h*CYP11B2) by LCI699 (IC_{50} = 0.2 nM). Although this inhibition contributed to the reduction of both systolic and diastolic blood pressures (10.0 and 6.0 mmHg, respectively), it, together with the twofold elevated adrenocorticotropic hormone in plasma that

Abbreviations: CYP, cytochrome P450; *h*CYP11B1, steroid 11*β*-hydroxylase; *h*CYP11B2, aldosterone synthase; *h*CYP17, 17*α*-hydroxylase-17,20-lyase; *h*CYP19, aromatase; SF, selectivity factor = $IC_{50\ hCYP11B2}/IC_{50\ hCYP11B1}$.

* Corresponding author. Pharmaceutical and Medicinal Chemistry, Saarland University, Campus C2 3, D-66123 Saarbrücken, Germany.
E-mail address: rolf.hartmann@helmholtz-hzi.de (R.W. Hartmann).

http://dx.doi.org/10.1016/j.ejmech.2015.04.013

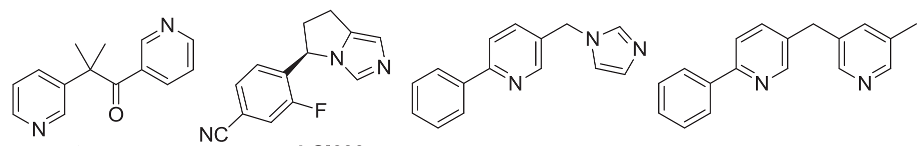

metyrapone **LCI699** **I** **II**

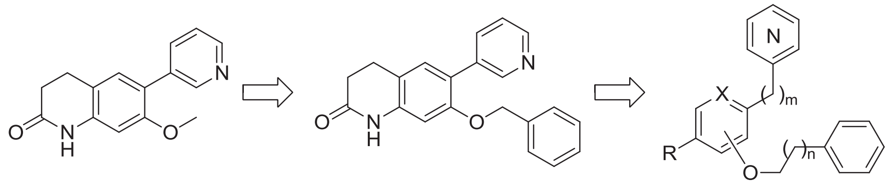

III
***h*CYP11B1** IC_{50} = 2487 nM
*h*CYP11B**2** IC_{50} = 268 nM
*h*CYP19 IC_{50} = 447 nM

IV
***h*CYP11B1** IC_{50} = 44 nM
*h*CYP11B**2** IC_{50} = 22 nM
*h*CYP19 IC_{50} = 35 nM
***r*CYP11B1** IC_{50} = 1500 nM

1 - 25
R = NO_2, ACNH, NH_2, 4-F PhCONH, OMe, F, H, $CONMe_2$, CF_3, CN;
X = C, N; m = 0, 1; n = 0-2

Chart 1. The structures of typical *h*CYP11B1 inhibitors (Metyrapone, LCI699, compounds **I** and **II**) as well as lead compounds **III**, **IV** and designed compounds **1**–**25**.

is the response to the drop of cortisol levels, boosted the concentrations of its precursor 11-deoxycorticosterone by 42-fold from 3.5 to 147.5 ng/dL. The binding of these over-produced 11-deoxycorticosterone to mineralocorticoid receptors induced around 8% reduction of the plasma potassium levels and consequently hypokalemia in one-third (4 out of 12) of patients. As evidenced by the decreased plasma renin levels (13–8 ng/L), which remained suppressed two weeks after the treatment discontinuation, the renin–angiotensin–aldosterone system was impaired. Therefore, the selectivity over *h*CYP11B2 is considered to be a crucial criterion for safety when treating Cushing's syndrome via *h*CYP11B1 inhibition. Besides this indication, topical application of *h*CYP11B1 inhibitors has also been proposed as a novel strategy to promote the healing of chronic wounds [11] based on the observation that cutaneously over-expressed cortisol impairs fibroblast proliferation and collagen synthesis, and thus induces chronic wounds and ulcers [12]. Cortisol also stimulates the proliferation of prostate cancer cells via certain mutated androgen receptors [13], therefore the combinatory application of *h*CYP11B1 inhibitors [14] or dual inhibitors of 17α-hydroxylase-17,20-lyase (*h*CYP17) and *h*CYP11B1 [15] could be superior approaches to improve the survival of prostate cancer patients. Since several other steroidogenic cytochrome P450 (CYP) enzymes including *h*CYP11B2, *h*CYP17 and aromatase (*h*CYP19) catalyze the biosynthesis of important steroidal hormones (mineralocorticoids, androgens and estrogens, respectively), drug candidates inhibiting *h*CYP11B1 ought to show adequate selectivity over these enzymes, in particular *h*CYP11B2 (as indicated by the results of the clinical trial of LCI699). The selectivity between *h*CYP11B1 and *h*CYP11B2 is especially challenging to achieve because of the high homology (>93%) between these two enzymes. Despite of this difficulty, potent and selective inhibitors of *h*CYP11B2 [16–21] were discovered recently. Aided by our broad experience in developing selective inhibitors of steroidogenic CYP enzymes, including *h*CYP11B2 [22–26], *h*CYP17 [27–33] and *h*CYP19 [34–38], several classes of potent *h*CYP11B1 inhibitors were identified [39–41]. Examples like compounds **I** (IC_{50} = 107 nM) [45] and **II** (IC_{50} = 2 nM) [41] exhibited both potent inhibition of *h*CYP11B1 (Chart 1 & Table 1) and promising selectivity over other CYP enzymes (for *h*CYP11B2, selectivity factors ($SF = IC_{50\ hCYP11B2}/IC_{50\ hCYP11B1}$) around 15 were observed). However, these compounds showed no (**I**, IC_{50} > 10,000 nM) to low (**II**, IC_{50} = 2440 nM) inhibition toward rat CYP11B1 (Table 1), which makes it difficult to prove the concept in rats. Therefore, discovery of compounds with novel structures inhibiting both human and rat CYP11B1 is necessary and urgent. In this study, we describe our efforts to identify new lead compounds exploiting previously acquired knowledge on developing selective inhibitors of steroidogenic CYP enzymes.

2. Results

2.1. Design concept

In our previous investigation of pyridyl substituted 3,4-dihydroquinolin-2(*1H*)-ones as potent inhibitors of *h*CYP11B2, an interesting SAR was observed that the bulkiness augment of the alkoxy substituent at the 7-position largely increased the *h*CYP11B1 inhibition [42]. The benzyloxy compound **IV** exhibited a 56-fold stronger *h*CYP11B1 inhibition than the corresponding methoxy analog **III** (IC_{50} = 2487 nM) with an IC_{50} value of 44 nM (Chart 1). Although the inhibition of *h*CYP11B2 was accordingly enhanced to 22 nM thus only showing an inadequate selectivity factor of 0.5 for *h*CYP11B1, a trend of reverse preference between *h*CYP11B1 and *h*CYP11B2 inhibition was anticipated when comparing it to that of compound **III** (SF = 0.1). More important is that compound **IV** showed a moderate inhibition of *r*CYP11B1 (IC_{50} = 1500 nM), which is apparently superior to the clinical used drug metyrapone (IC_{50} = 4607 nM) and the previously identified potent *h*CYP11B1 inhibitors **I** (IC_{50} > 10,000 nM) and **II** (IC_{50} = 2440 nM) (Chart 1 & Table 1). Due to the difficulty of identifying inhibitors of both human and rat CYP11B1 to facilitate the proof of concept in rats, compound **IV** was considered as a promising starting point for further modifications. However, as compound **IV** actually originated from a series of dual inhibitors of *h*CYP11B2 and *h*CYP19 [42,43], it showed significant inhibition of *h*CYP19 as well (IC_{50} = 35 nM). Therefore, besides elevating the potencies against human and rat CYP11B1, improvement of the selectivity over both *h*CYP11B2 and *h*CYP19 is another challenge encountered. To solve these problems, modifications were performed as shown in Chart 1. Since the 3,4-dihydroquinolin-2(*1H*)-one core was regarded as a privileged structure for *h*CYP11B2 inhibition [44], the lactam ring was opened and simplified into a phenyl substituted by various groups. As the insertion of a nitrogen atom into the core was demonstrated to be beneficial for the selectivity over *h*CYP11B2 [45], a pyridyl was also attempted replacing the benzene core. Based on the comparison between compounds **III** and **IV**, the

Table 1
Inhibition of *h*CYP11B1, *h*CYP11B2, *h*CYP19 and *r*CYP11B1 by compounds **1**–**25** as well as references **I**–**IV** and metyrapone.

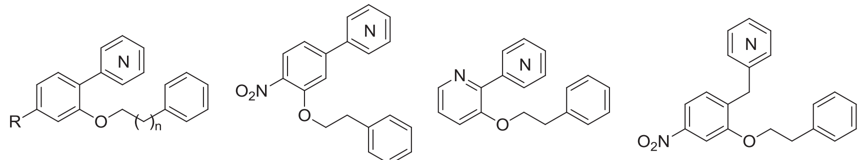

1 - 9, 12 - 21 **10, 11** **22, 23** **24, 25**

Compd.	Structure			IC_{50} (nM)[a]		SF[d]	IC_{50} (nM)[a]	
	R	Py	n	*h*CYP11B1[b]	*h*CYP11B2[b]		*h*CYP19[c]	*r*CYP11B1[b]
I				107	1423	13.3	>5000	>10,000
II				2	33	15.1	>5000	2440
III				2487	268	0.1	447	
IV				44	22	0.5	35	1500
Met[e]				15	72	4.9	>5000	4607
1	AcNH	3	0	279	643	2.3		
2	4-F PhCONH	3	0	1207	756	0.6		
3	NH_2	3	0	540	260	0.5		
4	NO_2	3	0	23	17	0.7	146	1493
5	NO_2	3	1	13	53	4.1	75	1307
6	NO_2	3	2	6	15	2.5	137	2083
7	NO_2	4	0	50	87	1.7	2425	648
8	NO_2	4	1	2	7	3.5	1894	163
9	NO_2	4	2	8	18	2.4	4993	370
10		3		508	447	0.9		
11		4		1201	714	0.6		
12	F	3	1	51	84	1.6		
13	F	4	1	60	74	1.2		
14	OMe	3	1	183	230	1.3		
15	OMe	4	1	46	70	1.5		
16	CF_3	3	1	812	945	1.2		
17	CF_3	4	1	26	24	0.9	2090	
18	CN	3	1	38	63	1.6	165	543
19	CN	4	1	12	23	1.9	1546	441
20	$CONMe_2$	3	1	594	299	0.5		
21	$CONMe_2$	4	1	1150	816	0.7		
22		3		1665	1453	0.9		
23		4		2665	2441	0.9		
24		3		182	246	1.3	128	706
25		4		6	16	2.7	157	2849

[a] Mean value of at least three experiments, standard deviation less than 25%.
[b] Hamster fibroblasts expressing *h*CYP11B1, *h*CYP11B2 or *r*CYP11B1, respectively; substrate deoxycorticosterone, 100 nM for *h*CYP11B1 and *h*CYP11B2 and 500 nM for *r*CYP11B1.
[c] human placental microsomes, substrate androstenedione, 500 nM.
[d] $SF = IC_{50\ hCYP11B2}/IC_{50\ hCYP11B1}$.
[e] Met: Metyrapone.

alkoxyl moiety was speculated to be a key for both potency and selectivity. The influences of the chain length and the substituting position of the alkoxyl group were therefore investigated. Since such kind of inhibitors competitively inhibit CYP enzymes via the coordination between their sp^2 hybrid N and the heme iron, the convenience to form these interactions, which largely depend on the relative position of the N with regard to the hydrophobic core, would exhibit significant impacts on both potency and selectivity. This factor was therefore examined by introducing either 3- or 4-pyridyl moieties as the heme-coordinating heterocycles as well as by inserting a methylene moiety between the pyridyl ring and the core, which have been found to alter the inhibitory pattern among steroidogenic CYP enzymes [11,39,43]. These efforts led to compounds **1**–**25** that were subsequently evaluated for their inhibition of both human and rat CYP11B1 as well as the selectivity over *h*CYP11B2, *h*CYP17 and *h*CYP19.

2.2. Chemistry

The syntheses of the designed compounds are shown in Schemes 1–3. For the majority of desired compounds, a straightforward general route was employed (Scheme 1). The starting bromo phenols that were substituted with various groups, such as NO_2, F, OMe, CF_3, CN and $CONMe_2$, were either commercially available or obtained from cleavage of the corresponding methoxy precursors. They were firstly alkylated using the corresponding bromines to afford ether intermediates **4a**–**6a**, **10a**, **12a**, **14a**, **16a**, **18a**, **20a** and **22a** before the 3- or 4-pyridyl moieties were introduced via Suzuki coupling reaction resulting in final compounds **4**–**23**. This reaction sequence was established after having observed low yields of alkylation with pyridyl substituted phenols. In most cases, the ordinary Suzuki coupling condition, i.e. boiling the corresponding reactants with $Pd(PPh_3)_4$ and Na_2CO_3 in a mixture of ethanol, toluene and water, gave satisfying yields; while, for compounds **10**–**13**, **18**, **19** and **23**, $PdCl_2(dppf)$ had to be employed as an alternative. The nitro group in compound **4** was reduced to amino (**3**) using hydrazine hydrate and Pd/C, which was further acylated with acetyl chloride or 4-fluorobenzoyl chloride to obtain final compounds **1** and **2**, respectively. To achieve the introduction of a methylene moiety between the pyridyl and the benzene core, the bromo group in **5a** was first converted into borate (**24a**) using bis(pinacolato)diboron under the catalysis of

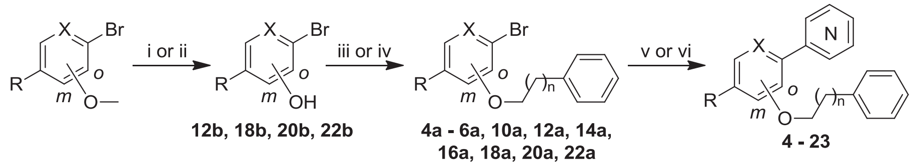

	R	X	OR'	n	Py
4	NO_2	C	*o*	0	3
5	NO_2	C	*o*	1	3
6	NO_2	C	*o*	2	3
7	NO_2	C	*o*	0	4
8	NO_2	C	*o*	1	4
9	NO_2	C	*o*	2	4
10	NO_2	C	*m*	1	3
11	NO_2	C	*m*	1	4
12	F	C	*o*	1	3
13	F	C	*o*	1	4
14	OMe	C	*o*	1	3
15	OMe	C	*o*	1	4
16	CF_3	C	*o*	1	3
17	CF_3	C	*o*	1	4
18	CN	C	*o*	1	3
19	CN	C	*o*	1	4
20	$CONMe_2$	C	*o*	1	3
21	$CONMe_2$	C	*o*	1	4
22	H	N	*o*	1	3
23	H	N	*o*	1	4

variables in intermediates are the same as those in the corresponding final compounds

Scheme 1. Syntheses of compounds **4**–**23**. Reagents and conditions. (i) Method A: BBr_3, DCM, −20 to RT, overnight. (ii) for **22b**: HBr, 140 °C, overnight. (iii) Method B: corresponding brimide, K_2CO_3, KI, ethanol, reflux, overnight. (iv) for **10a**: (2-bromoethyl)benzene, tetrabutylammonium iodide, DMF, Cs_2CO_3, 140 °C, 3 h. (v) for **4**–**9**, **14**–**17** and **20**–**22**: Method C: $Pd(PPh_3)_4$, corresponding pyridylboronic acid, Na_2CO_3, ethanol, toluene, H_2O, reflux, 3–5 h. (vi) for **10**–**13**, **18**, **19** and **23**: Method D: $PdCl_2(dppf)$, corresponding pyridylboronic acid, Na_2CO_3, DME, H_2O, reflux, overnight.

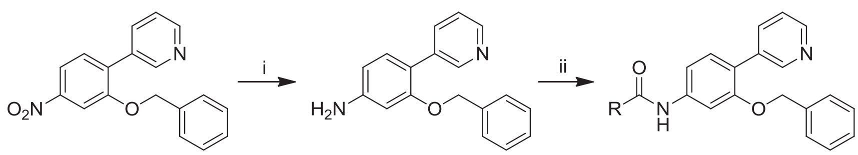

4 **3** **1**: Me, **2**: 4-F Ph

Scheme 2. Syntheses of compounds **1**–**3**. Reagents and conditions. (i) hydrazine hydrate, Pd/C, EtOH, reflux, 1 h. (ii) acetyl chloride or 4-fluorobenzoyl chloride, triethylamine, *N*,*N*-dimethylamionpyridine, dichloromethane, RT, overnight.

$PdCl_2(PPh_3)_2$, which subsequently coupled with 3- or 4-(bromomethyl)pyridine to yield compounds **24** and **25**, respectively.

2.3. Biological results and discussions

2.3.1. Inhibition of hCYP11B1 and hCYP11B2

The synthesized compounds **1**–**25** were tested for their inhibition of *h*CYP11B1 and *h*CYP11B2 in V79MZ cells expressing the corresponding enzymes, respectively, with [^{3}H]-11-deoxycorticosterone as substrate [46]. Results are presented in Table 1 with metyrapone and compound **I**–**IV** as references.

The 3,4-dihydroquinolin-2(*1H*)-one core in the lead compound **IV** was opened as the first step of modification because this structure was regarded as a privileged structure for *h*CYP11B2 inhibition [44]. In contrast, the 3-pyridyl was left untouched to ensure direct comparisons of inhibitory potencies. The lactam ring was simplified into an acetamido group substituting the benzene core to maintain potential hydrogen bonds formed by the amide group. As expected, the resulting compound **1** exhibited preference for *h*CYP11B1 inhibition with a SF of 2.3, which is around 5-fold better than that of the lead compound **IV**. However, its *h*CYP11B1 inhibition was simultaneously reduced to 279 nM. A bulky 4-fluorobenzamido group (**2**) further decreased the inhibitory potency by 4-fold—1207 nM. This observation is probably a result of steric clashes caused by increased bulkiness and/or rotation freedom after removing the astriction of the lactam ring. The replacement of amido groups by an amino moiety (**3**) only led to a moderate inhibition of *h*CYP11B1 ($IC_{50} = 540$ nM). Surprisingly, the nitro analog **4** showed potent *h*CYP11B1 inhibition with an IC_{50} value of 23 nM, which is twice as potent as the lead **IV** (IC_{50} = 44 nM). However, compound **4** failed to exhibit any superiority to lead **IV** regarding selectivity over *h*CYP11B2 (SF = 0.7). With the nitro group sustained, the influence of the chain length of the alkoxyl moiety was subsequently investigated. As the augmentation of methylene units, the inhibition of *h*CYP11B1 was elevated from 23 nM (**4**, n = 0, benzoxy) to 13 nM (**5**, n = 1) and to 6 nM (**6**, n = 2). Despite of the fact that all compounds also showed potent inhibition of *h*CYP11B2, improvements of selectivity compared to lead compound **IV** (SF = 0.5) was achieved, in particular for compound **5**, which exhibited a SF of 4.1. The displacement of 3-pyridyl by 4-pyridyl did not influence much the inhibitory potency of *h*CYP11B1. The corresponding benzoxy compound **7** was also a potent inhibitor with an IC_{50} value of 50 nM. With the insertion of more methylene units, a similar increase of inhibitory potency was observed. Phenethoxy analog **8** (n = 1, IC_{50} = 2 nM) was 25-fold more potent than the benzoxy compound **7**; while an IC_{50} of 8 nM was observed for the phenylpropoxy compound **9**. Being the most potent *h*CYP11B1 inhibitor in this study, compound **8** was 22- and 7-fold more potent than the lead compound **IV** and metyrapone, respectively, and also exhibited a similar selectivity over

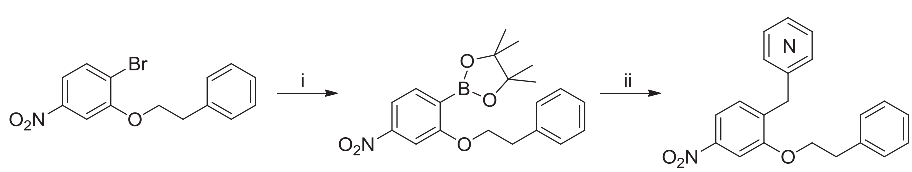

5a **24a** **24**: 3-Py, **25**: 4-Py

Scheme 3. Syntheses of compounds **24** and **25**. Reagents and conditions. (i) bis(pinacolato)diboron, $PdCl_2(PPh_3)_2$, KOAc, dioxane, reflux, 4 h. (ii) Method D: $PdCl_2(dppf)$, corresponding pyridylboronic acid, Na_2CO_3, DME, H_2O, reflux, 4 h.

*h*CYP11B2 as metyrapone. The fact that both 3- and 4-pyridyl compounds showed similar potency is an indication of a relative large pocket, in which the benzene cycle could drift a bit to provide the suitable angle to form the N–Fe coordination. The high flexibility of the alkoxyl side chain could enable the compounds to adapt to the angle change. In contrast, the position of the alkoxyl group was obviously more decisive for *h*CYP11B1 inhibition. The shift from the ortho-(with regard to the pyridyl) to the meta-position resulted in deceases of potency by 85- and 600-fold for the 3- and 4-pyridyl analogs (**10**, IC_{50} = 508 nM; and **11**, IC_{50} = 1201 nM), respectively. Since phenethoxy analogs showed better selectivity (SF of 4.1 for compound **5** and 3.5 for compound **8**), this chain length was sustained in the subsequent modifications. In contrast, both 3- and 4-pyridyl analogs were synthesized to avoid missing any potential strong inhibitors. Although nitro groups present in a considerable number of drugs in clinical use, such as nifedipine, they have the potential of being reduced to aromatic nitrosos, which can covalently binds to DNA and proteins, and thus are carcinogenic [47]. Wariness was therefore put on the nitro groups and the replacement of nitro by other substituents was attempted. When relatively small groups were introduced into the molecules (F in **12** & **13**; OMe in **15**; CF_3 in **17**; and CN in **18** & **19**), potent *h*CYP11B1 inhibition was observed with IC_{50} values less than 60 nM. CN in combination with 4-pyridyl led to the most potent compound in this small set with an IC_{50} value of 12 nM. An exception is OMe in the 3-pyridyl compound **14**, which showed a moderate *h*CYP11B1 inhibition (IC_{50} = 183 nM); whereas CF_3 in combination with 3-pyridyl surprisingly only resulted in a weak inhibitory potency (IC_{50} = 812 nM). Accordingly, the bulkier $CONMe_2$ substituents led to weak inhibition with IC_{50} values of 594 and 1150 nM for 3-Py (**20**) and 4-Py (**21**) compounds, respectively, indicating potential steric hindrances. In contrast to bulkiness, other properties, such as electrostatic potential and the ability to form hydrogen bonds, seem to play only minor roles. When the substituent is as small as F, no significant difference in potency was found between 3- and 4-pyridyl compounds **12** and **13** (IC_{50} values of 51 and 60 nM, respectively); while for other groups with larger size (OMe, CF_3 and CN in compounds **14**–**19**), the 4-pyridyl analogs were significantly more potent than the corresponding 3-pyridyl compounds. Although more potent *h*CYP11B1 inhibitors were identified via these replacements, no improvement of selectivity over *h*CYP11B2 was observed (SFs < 2). As the replacement of the benzene core by a pyridyl moiety in the biaryl methylene substituted heterocycle class of *h*CYP11B1 inhibitors increased the selectivity over *h*CYP11B2 [45], a nitrogen atom was inserted into the benzene core leading to compounds **22** and **23**. However, this modification strongly reduced the *h*CYP11B1 inhibition (IC_{50} > 1400 nM). Moreover, the introduction of a methylene moiety between the benzene core and the 3-pyridyl group (**24**) decreased the potency by around 10-fold compared to the corresponding analog **5**; whereas the same modification on 4-pyridyl compound **25** led to a potent *h*CYP11B1 inhibitor with similar potency (IC_{50} = 6 nM) as the parent compound **8**.

2.3.2. Inhibition of human CYP17 and CYP19

Since this series of compounds were originated from the lead compound **IV**, which showed a potent inhibition of *h*CYP19 (IC_{50} = 35 nM), the improvement of the corresponding selectivity was a tough task throughout the modifications. The most potent *h*CYP11B1 inhibitors **4**–**9**, **17**–**9**, **24** and **25** were therefore evaluated for their inhibition of *h*CYP19 with human placental microsomes using [1β-^{3}H]androstenedione (500 nM) as a substrate [48]. Apparently, all 3-pyridyl compounds (**4**–**6**, **18** and **24**) exhibited potent inhibition of *h*CYP19 with IC_{50} values below 170 nM (Table 1). In contrast, 4-pyridyl analogs (**7**–**9**, **17** and **29**) showed very weak to no inhibition toward *h*CYP19 with IC_{50} values ranging from 1500 to 5000 nM. The only exception was compound **25** (IC_{50} = 157 nM) probably due to the methylene moiety between the heme-coordinating pyridyl and the benzene core. With an improvement of more than 40-fold on *h*CYP19 selectivity compared to lead **IV**, these 4-pyridyl compounds are not likely to reduce estrogen biosynthesis under the treatment doses when taking into consideration their very strong inhibitory potency against the target enzyme *h*CYP11B1.

Since *h*CYP17 is of crucial importance for the production of androgens, the selectivity over this steroidogenic enzyme was employed as another criterion for safety. The above-mentioned compounds were further investigated for their *h*CYP17 inhibition using the 50,000 g sediment of an *Escherichia coli* homogenate recombinantly expressing *h*CYP17 with progesterone (25 μM) as a substrate [49]. No inhibition (IC_{50} > 10 μM) was observed for all compounds tested indicating safety with regard to this aspect.

2.3.3. Inhibition of rat CYP11B1

As one of the major tasks of this study, the inhibition of *r*CYP11B1 was determined for the most potent inhibitors of the human enzyme (same as mentioned in the last section) in V79MZ cells expressing *r*CYP11B2 [50]. Interestingly, for nitro compounds, all 4-pyridyl analogs **7**–**9** (IC_{50} < 650 nM) were much stronger than 3-pyridyl compounds **4**–**6** (IC_{50} ranging from 1300 to 2000 nM). Compound **8** as the most potent one exhibited an IC_{50} value of 163 nM, which was near 10- and 28-fold stronger than lead **IV** and metyrapone, respectively. In contrast, when substituted with CN, no significant difference in potency between 3- and 4-pyridyl compounds **18** and **19** was observed (IC_{50} around 500 nM); whereas, in the case of methylene compounds, the 4-pyridyl derivative **25** showed an about 4-fold weaker inhibition compared to the corresponding 3-pyridyl compound **24** (IC_{50} of 2850 vs 706 nM), which is in contrast to the SAR observed with the nitro compounds.

2.3.4. Modeling studies

To further investigate the interactions between the synthesized inhibitors and the targeting enzyme, a homology model of human CYP11B1 was established using the reported crystal structure of *h*CYP11B2 as the template. The sequences of both *h*CYP11B1 (UniProt code: P15538) and *h*CYP11B2 (UniProt code: P19099) comprise 503 amino acids, among which 473 are identical (Figure S1). In the crystal of *h*CYP11B2 in complex with deoxycorticosterone (PDB ID: 4DVQ, chain A), amino acids 34-502 present. Since amino acids 1–24 as a transit peptide is less relevant to biological functions and configuration, amino acids 1–33 in the *h*CYP11B1 sequence was omitted similar as in the template crystal when establishing the model. A library of ten models was initially generated and the best one was selected according to electrostatic solvation energy and root mean square deviation of each intermediate model to the average position of all models. This preliminary model was subsequently further refined via molecular dynamic simulation to yield the final one. The quality of the resulting homology model was evaluated regarding the stereochemical measurements of each amino acid including bond lengths, angles, dihedrals and φ–ψ torsions. As shown in the Ramachandran scatter plot (Figure S2), 451 out of 470 amino acid (96%) clustered in favorable regions, whereas only one amino acid (Ser288) was considered as an outlier (0.2%). This *h*CYP11B1 homology model presented characteristic cytochrome P450 folds and nicely superposed to the template structure (Fig. 1A). Although 30 amino acids differ in the sequences of these two enzymes, they locate outside the active sites. It is therefore not surprising that the configuration of their active sites are very similar. However, a scrutiny on the active sites still revealed minor differences (Fig. 1B), which could be the basis and keys for inhibitors to selectively inhibit an individual enzyme. In the *h*CYP11B1 homology model, the middle part of the I-helix extruded slightly toward the opposite β2-sheet compared to that in the *h*CYP11B2 crystal thus narrowing the binding pocket; while the F-helix and the heme moiety as the roof and the floor of the active site, respectively, subsided by around 2 Å synchronously. Although drifts were also observed for the β2-sheet, the B–B′ loop and the (β4-1)-(β4-2) loop, alterations were identified in the B′-C loop that are subtle nevertheless of greater importance in changing the binding site (Fig. 1C). The side chain of Leu131 jostled toward the β2-sheet thus shrinking the hydrophobic pocket in between. In contrast, the phenyl group of Phe130 turned downward to heme moiety leading to more convenience for inhibitors to enter and exploit this pocket. The most promising compound (**8**) in this study was subsequently docked into the *h*CYP11B1 homology model to investigate the interactions between inhibitors and targeting enzyme. The molecule was anchored by the coordination between the sp^2 hybrid N in pyridyl and the heme iron and leaned on the β2-sheet with an angle of approximate 60° with respect to the heme plane (Fig. 2A). The phenethoxyl group stretched out pointing to the B–B′ loop and fitted into the hydrophobic pocket mentioned above, which was delimitated by Arg110–Met111–Ser112–Leu113–Leu131–Glu383 (Fig. 2B). The phenyl side chains of Phe130 and Phe381 served as two gates of this pocket and formed π–π interactions with the phenethoxyl group in parallel and perpendicular manners, respectively. An arene–cation interaction was also observed between the phenethoxyl substituent and the guanidyl of Arg110. Since the side chains of Glu383 and Met111 were accessible, the introduction of positive-charged groups and/or hydrogen bond donors onto the phenethoxyl moiety to form salt bridge and/or hydrogen bond would elevate inhibitory potency. As this pocket in *h*CYP11B1 homology model exhibited a more convenient entrance (Phe130) but a reduced volume (Leu131) compared to that in the *h*CYP11B2 crystal structure, this feature could be exploited to achieve more selectivity. Furthermore, Phe130 and Phe381 formed π–π interactions with the pyridyl moiety (parallel) and the phenyl core (perpendicular) and thus promoted affinity and stabilized the binding pose. An additional π–π interaction between Phe487 and the phenyl core (parallel) as well as hydrogen bonds formed by the nitro group with Tyr485 and Leu380 also contributed significantly with this regard. The drift of I-helix toward the β2-sheet narrowing the active site possibly facilitated the formation of these hydrogen bonds, but also increased the risks of steric clashes for bulkier substituents, which is in accordance with the SAR discussed above.

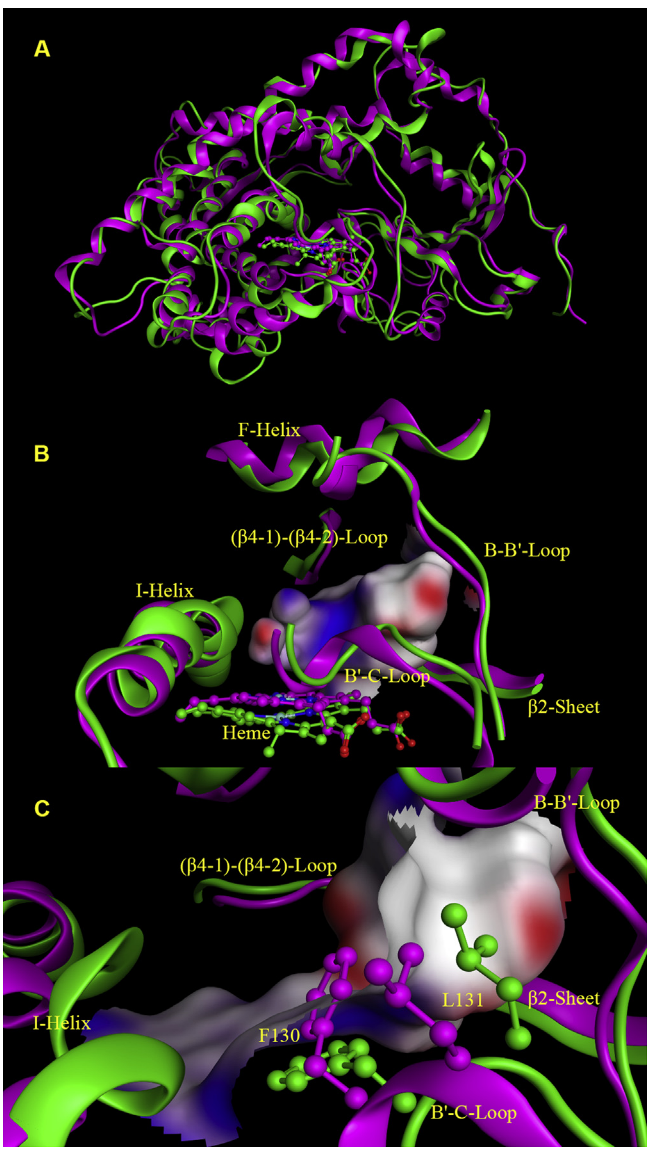

Fig. 1. (A) Superposition of the *h*CYP11B1 homology model (green) onto the *h*CYP11B2 crystal structure (magenta, PDB ID: 4DVQ-A). (B) Comparison of the active sites. (C) Configurational changes of F130 and L131 strongly influenced the hydrophobic pocket delimitated by B′-C loop, B–B′ loop and β2-sheet. (For interpretation of the references to colour in this figure legend, the reader is referred to the web version of this article.)

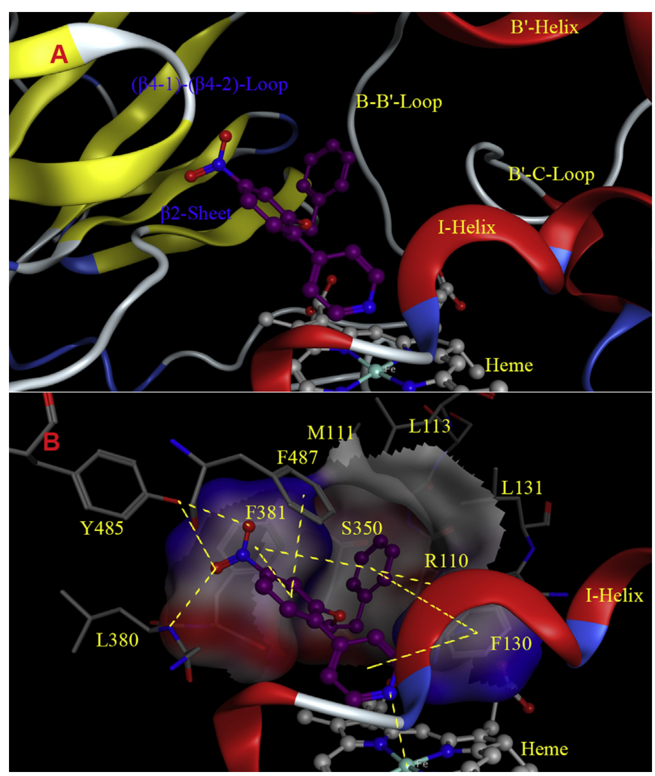

Fig. 2. Docking of compound **8** (magenta) in the *h*CYP11B1 homology model. Interactions between the inhibitor and the enzyme are depicted in gold dashed lines. (For interpretation of the references to colour in this figure legend, the reader is referred to the web version of this article.)

3. Conclusions

As evidenced by the clinical application of metyrapone and the phase I clinical study of LCI699, the inhibition of *h*CYP11B1 is an elegant approach to treat Cushing's syndrome, in particular for the recurrent and subclinical cases. To overcome the inconvenience in achieving proof of concept in rats, which is caused by the impotency of our previously discovered *h*CYP11B1 inhibitors against the corresponding rat enzyme, efforts were paid to identify novel lead compounds with different structures. Modifications on a potent promiscuous inhibitor (**IV**) of *h*CYP11B1, *h*CYP11B2 and *h*CYP19 (IC_{50} values of 44, 22 and 35 nM, respectively) that exhibited moderate *r*CYP11B1 inhibition (IC_{50} = 1500 nM) led to compound **8** as a new promising lead compound. Compared to the starting point compound **IV**, this inhibitor showed not only 22- and 9-fold elevations on both human and rat CYP11B1 inhibition with IC_{50} values of 2 and 163 nM, respectively, but also significant improvement of selectivity over *h*CYP19 (54-fold, IC_{50} = 1900 nM). Accordingly, compound **8** was around 7- and 28-fold more potent than the drug metyrapone regarding the inhibition of human and rat CYP11B1. Although its selectivity over *h*CYP11B2 was also increased by a factor of 7 (SF of 3.5 vs 0.5) compared to compound **IV** reaching a similar level as metyrapone (SF = 4.9), it was considered insufficient and remains to be improved. With further optimizations on the new lead compound **8** that was successfully identified in this study, drug candidates with satisfying profiles are expected to be discovered for the consequent drug development and the research of pathophysiology involving CYP11B1.

4. Experimental section

4.1. Chemistry

4.1.1. Chemical and analytical methods

Melting points were measured on a Mettler FP1 melting point apparatus and are uncorrected. ^{1}H NMR and ^{13}C NMR were recorded on a Bruker AM500 spectrometer at 500 MHz and 125 MHz, respectively, at 300 K. Chemical shifts are reported in parts per million (ppm), by reference to the hydrogenated residues of the deuterated solvent as internal standard. All coupling constants (*J*) are given in Hertz (*Hz*). Mass spectra (LC/UV/MS: ESI) were recorded on a SpectraSystem/MSQ Plus (ThermoFinnigan) instrument with a RP18-100-5 column (Macherey–Nagel). A water/acetonitrile gradient was used as eluent system. All compounds are >95% chemical pure as measured by LC/UV trace at 254 nm. Reagents were used as obtained from commercial suppliers without further purification. Solvents were distilled before use. If necessary, solvents were dried by distillation from appropriate drying reagents prior to use. Flash chromatography was performed on silica gel 40 (35/40–63/70 μM) with petroleum ether/ethyl acetate or CH_2Cl_2/methanol mixtures as eluents. Reaction progress was monitored by thin-layer chromatography (TLC) on TLC Silica Gel 60 F_{254} (Merck KGaA). Visualization was accomplished with UV light.

4.1.2. General procedure A: methoxyl cleavage with boron tribromide

A solution of the corresponding methoxyl starting material in DCM (4 mL/mmol) was cooled to −20 °C before boron tribromide (3 eq, 1 M in DCM) was added in a nitrogen atmosphere at the same temperature. The stirred solution was subsequently warmed to ambient temperature overnight. The resulted reaction mixture was diluted with water and the phases were separated. The aqueous layer was extracted three times with ethyl acetate and the combined organic layers were dried over Na_2SO_4. The solvent was removed under reduced pressure and the crude product was purified by flash chromatography on silica gel.

4.1.3. General procedure B: etherization

To the corresponding bromophenol in ethanol (5 mL/mmol) was added K_2CO_3 (1.2 eq). The resulted mixture was stirred for 2 h under reflux conditions (90 °C) before the corresponding bromide (1.3 eq) and KI (5 mol%) were added. Reflux was continued overnight. After cooling down, the solvent was removed under reduced pressure and the residue was washed with brine and extracted three times with ethyl acetate. The combined organic layers were dried over Na_2SO_4, the solvent was removed under reduced pressure and the crude product was purified by flash chromatography on silica gel.

4.1.4. General procedure C: Suzuki coupling catalyzed by $Pd(PPh_3)_4$

The corresponding bromide (1.0 eq) and pyridylboronic acid (1.5 eq) were dissolved in a mixture of ethanol (10 mL/100 mg), toluene (10 mL/100 mg) and an aqueous 2.0 M Na_2CO_3 solution (2.5 mL/100 mg). The mixture was deoxygenated and flushed with nitrogen three times before $Pd(PPh_3)_4$ (5 mol%) was added. The resulting suspension was heated under reflux for 3–5 h. After cooling down, water and ethyl acetate were added and the phases were separated. The water phase was extracted three times with ethyl acetate and the combined organic layers were dried over Na_2SO_4. The solvent was removed under reduced pressure and the crude product was purified by flash chromatography on silica gel.

4.1.5. General procedure D: Suzuki coupling catalyzed by $PdCl_2$(dppf)

The corresponding bromide (1.0 eq) and pyridylboronic acid (1.5 eq) were dissolved in a mixture of DME (10 mL/100 mg) and an aqueous 2.0 M Na_2CO_3 solution (2.5 mL/100 mg). The mixture was deoxygenated and flushed with nitrogen three times before $PdCl_2$(dppf) (5 mol%) was added. The resulting suspension was heated under reflux for 3–5 h or overnight. After cooling down, water and ethyl acetate were added and the phases were separated. The water phase was extracted three times with ethyl acetate and the combined organic layers were dried over Na_2SO_4. The solvent was removed under reduced pressure and the crude product was purified by flash chromatography on silica gel.

4.1.6. N-(3-(benzyloxy)-4-(pyridin-3-yl)phenyl)acetamide (*1*)

To the solution of 3-(benzyloxy)-4-(pyridin-3-yl)aniline **3** (100 mg, 0.36 mmol), triethylamine (0.10 mL, 0.72 mmol) and *N*,*N*-dimethylpyridin-4-amine (2 mg) in dicholoromathane (20 mL) was dropped in acetyl chloride (29.8 mg, 0.38 mmol) in an ice bath. The resulting reaction mixture was subsequently stirred at room temperature overnight before water (20 mL) was added and the phases were separated. The water phase was extracted three times with dicholoromathane (10 mL) and the combined organic layers were dried over Na_2SO_4. The solvent was removed under reduced pressure and the crude product was purified by flash chromatography on silica gel using a mixture of dicholromethane/methanol (50:1) as eluent. Yield: 109 mg (95%); yellow solid: mp 157–159 °C; R_f = 0.29 (n-Hex/EtOAc 1:2); Anal. $C_{20}H_{18}N_2O_2$ (C, H, N, O). ^{1}H NMR ($CDCl_3$, 500 MHz): δ_H = 8.78 (d, *J* = 1.7 Hz, 1H), 8.54 (dd, *J* = 1.7, 4.8 Hz, 1H), 7.87–7.89 (m, 1H), 7.47 (d, *J* = 1.7 Hz, 1H), 7.37 (s, br, 1H), 7.31–7.34 (m, 1H), 7.24–7.27 (m, 3H), 7.15–7.18 (m, 1H), 7.10–7.12 (m, 2H), 6.97 (dd, *J* = 1.9, 8.2 Hz, 1H), 4.79 (s, 2H), 2.20 (s, 3H); ^{13}C NMR ($CDCl_3$, 125 MHz): δ_C = 156.4, 150.1, 147.7, 141.3, 139.3, 136.8, 136.7, 133.9, 130.6, 128.4, 125.9, 123.0, 122.8, 111.7, 104.3, 70.4, 20.5; MS (ESI): *m*/*z* = 319.14 [M+H]$^+$.

4.1.7. N-(3-(benzyloxy)-4-(pyridin-3-yl)phenyl)-4-fluorobenzamide (**2**)

To the solution of 3-(benzyloxy)-4-(pyridin-3-yl)aniline **3** (100 mg, 0.36 mmol), triethylamine (0.10 mL, 0.72 mmol) and *N,N*-dimethylpyridin-4-amine (2 mg) in dicholoromathane (20 mL) was dropped in 4-fluorobenzoyl chloride (60.0 mg, 0.38 mmol) in an ice bath. The resulting reaction mixture was subsequently stirred at room temperature overnight before water (20 mL) was added and the phases were separated. The water phase was extracted three times with dicholoromathane (10 mL) and the combined organic layers were dried over Na_2SO_4. The solvent was removed under reduced pressure and the crude product was purified by flash chromatography on silica gel using a mixture of dicholromethane/methanol (50:1) as eluent. Yield: 130 mg (91%); yellow solid: mp 166–167 °C; $R_f = 0.35$ (n-Hex/EtOAc 1:2); Anal. $C_{25}H_{19}FN_2O_2$ (C, H, N, O). ^1H NMR ($CDCl_3$, 500 MHz): $\delta_H = 8.82$ (d, $J = 1.7$ Hz, 1H), 8.63 (dd, $J = 1.7$, 4.8 Hz, 1H), 8.10 (dd, $J = 1.9$, 8.2 Hz, 2H), 7.92–7.94 (m, 1H), 7.65 (d, $J = 1.7$ Hz, 1H), 7.59 (s, br, 1H), 7.24–7.35 (m, 6H), 7.17–7.22 (m, 3H), 6.95 (m, 1H), 4.76 (s, 2H); ^{13}C NMR ($CDCl_3$, 125 MHz): $\delta_C = 159.7$ (d, $J_{CF} = 245.7$ Hz), 154.7, 147.3, 138.8, 137.9, 134.7, 126.9, 123.4, 119.8 (d, $J_{CF} = 10.1$ Hz), 119.7 (d, $J_{CF} = 10.6$ Hz), 119.2, 118.9, 118.7, 117.2, 117.1, 114.0, 111.1, 105.8 (d, $J_{CF} = 26.6$ Hz), 105.6 (d, $J_{CF} = 26.1$ Hz), 103.7, 102.0, 71.5; MS (ESI): $m/z = 399.14$ $[M+H]^+$.

4.1.8. 3-(Benzyloxy)-4-(pyridin-3-yl)aniline (**3**)

To the suspension of 3-(2-(benzyloxy)-4-nitrophenyl)pyridine **4** (25 mg, 0.08 mmol) and Pd/C (2.2 mg, 10% mmol) in ethanol (5 mL) was added hydrazine hydrate (11.2 mg, 0.25 mmol) slowly in an ice bath. The resulting reaction mixture was subsequently heated to reflux for 1 h. After cooling down to room temperature, water (10 mL) and ethyl acetate (10 mL) were added and the phases were separated. The water phase was extracted three times with ethyl acetate (10 mL) and the combined organic layers were dried over Na_2SO_4. The solvent was removed under reduced pressure and the crude product was purified by flash chromatography on silica gel using a mixture of dicholromethane/methanol (50:1) as eluent. Yield: 19 mg (86%); yellow solid: mp 172–174 °C; $R_f = 0.21$ (n-Hex/EtOAc 1:2); Anal. $C_{18}H_{16}N_2O$ (C, H, N, O). ^1H NMR ($CDCl_3$, 500 MHz): $\delta_H = 8.67$ (d, $J = 2.6$ Hz, 1H), 8.47 (dd, $J = 1.7$, 4.8 Hz, 1H), 7.65–7.67 (m, 1H), 7.26–7.29 (m, 2H), 7.15–7.17 (m, 2H), 7.09 (d, $J = 8.1$ Hz, 1H), 6.35 (dd, $J = 2.1$, 8.1 Hz, 1H), 6.30 (d, $J = 2.1$ Hz, 1H), 4.79 (s, 2H), 3.85 (s, br, 2H, NH_2); ^{13}C NMR ($CDCl_3$, 125 MHz): $\delta_C = 156.9$, 150.0, 147.9, 146.9, 136.7, 134.4, 129.0, 128.4, 126.5, 122.6, 117.5, 107.6, 99.4, 70.4; MS (ESI): $m/z = 277.13$ $[M+H]^+$.

4.1.9. 3-(2-(Benzyloxy)-4-nitrophenyl)pyridine (**4**)

The title compound was synthesized from 2-(benzyloxy)-1-bromo-4-nitrobenzene **4a** (108 mg, 0.35 mmol) according to method C using 3-pyridylboronic acid. The crude product was purified by flash chromatography on silica gel using a mixture of petroleum ether/ethyl acetate (2:1) as eluent. Yield: 80 mg (75%); lemon yellow solid: mp 121–123 °C; $R_f = 0.37$ (n-Hex/EtOAc 1:2); Anal. $C_{18}H_{14}N_2O_3$ (C, H, N, O). ^1H NMR ($CDCl_3$, 500 MHz): $\delta_H = 8.71$ (d, $J = 1.9$ Hz, 1H), 8.53 (dd, $J = 1.4$, 4.8 Hz, 1H), 7.85–7.88 (m, 2H), 7.79–7.81 (m, 1H), 7.40 (d, $J = 8.2$ Hz, 1H), 7.23–7.28 (m, 6H), 5.12 (s, 2H); ^{13}C NMR ($CDCl_3$, 125 MHz): $\delta_C = 156.0$, 150.0, 149.3, 148.6, 136.8, 135.3, 134.2, 132.2, 131.0, 128.8, 128.4, 127.1, 123.0, 116.5, 107.9, 71.1; MS (ESI): $m/z = 307.10$ $[M+H]^+$.

4.1.10. 3-(4-Nitro-2-phenethoxyphenyl)pyridine (**5**)

The title compound was synthesized from 1-bromo-4-nitro-2-phenethoxybenzene **5a** (175 mg, 0.54 mmol) according to method C using 3-pyridylboronic acid. The crude product was purified by flash chromatography on silica gel using a mixture of petroleum ether/ethyl acetate (2:1) as eluent. Yield: 137 mg (78%); yellow solid: mp 125–126 °C; $R_f = 0.39$ (n-Hex/EtOAc 1:2); Anal. $C_{19}H_{16}N_2O_3$ (C, H, N, O). ^1H NMR ($CDCl_3$, 500 MHz): $\delta_H = 8.77$ (s, 1H), 8.72 (d, $J = 4.8$ Hz, 1H), 8.00 (d, $J = 8.3$ Hz, 1H), 7.90 (s, 1H), 7.75 (d, $J = 7.9$ Hz, 1H), 7.52 (d, $J = 8.3$ Hz, 1H), 7.31–7.41 (m, 4H), 7.23 (d, $J = 7.4$ Hz, 2H), 4.40 (t, $J = 6.5$ Hz, 2H), 3.15 (t, $J = 6.5$ Hz, 2H); ^{13}C NMR ($CDCl_3$, 125 MHz): $\delta_C = 156.3$, 149.9, 149.2, 148.5, 137.6, 136.9, 133.8, 132.2, 130.9, 129.0, 128.5, 126.7, 122.9, 116.1, 107.0, 69.9, 35.4; MS (ESI): $m/z = 321.12$ $[M+H]^+$.

4.1.11. 3-(4-Nitro-2-(3-phenylpropoxy)phenyl)pyridine (**6**)

The title compound was synthesized from 1-bromo-4-nitro-2-phenethoxybenzene **6a** (125 mg, 0.37 mmol) according to method C using 3-pyridylboronic acid. The crude product was purified by flash chromatography on silica gel using a mixture of petroleum ether/ethyl acetate (2:1) as eluent. Yield: 89 mg (72%); yellow solid: mp 117–119 °C; $R_f = 0.37$ (n-Hex/EtOAc 1:2); Anal. $C_{20}H_{18}N_2O_3$ (C, H, N, O). ^1H NMR ($CDCl_3$, 500 MHz): $\delta_H = 8.79$ (d, $J = 41.5$ Hz, 1H), 8.62 (dd, $J = 1.5$, 4.8 Hz, 1H), 7.92 (dd, $J = 2.1$, 8.4 Hz, 1H), 7.87 (dt, $J = 1.8$, 7.9 Hz, 1H), 7.77 (d, $J = 2.1$ Hz, 1H), 7.45 (d, $J = 8.3$ Hz, 1H), 7.36–7.39 (m, 1H), 7.23–7.25 (m, 2H), 7.15–7.18 (m, 2H), 7.08 (d, $J = 7.0$ Hz, 2H), 4.07 (t, $J = 6.2$ Hz, 2H), 2.68 (t, $J = 7.3$ Hz, 2H), 2.06–2.09 (m, 2H); ^{13}C NMR ($CDCl_3$, 125 MHz): $\delta_C = 156.6$, 150.3, 149.5, 148.9, 141.0, 137.0, 134.1, 132.6, 131.1, 128.8, 128.6, 126.4, 123.2, 116.4, 107.4, 68.4, 32.3, 30.7; MS (ESI): $m/z = 335.13$ $[M+H]^+$.

4.1.12. 4-(2-(Benzyloxy)-4-nitrophenyl)pyridine (**7**)

The title compound was synthesized from 2-(benzyloxy)-1-bromo-4-nitrobenzene **4a** (150 mg, 0.49 mmol) according to method C using 4-pyridylboronic acid. The crude product was purified by flash chromatography on silica gel using a mixture of petroleum ether/ethyl acetate (2:1) as eluent. Yield: 107 mg (72%); yellow solid: mp 129–121 °C; $R_f = 0.33$ (n-Hex/EtOAc 1:2); Anal. $C_{18}H_{14}N_2O_3$ (C, H, N, O). ^1H NMR ($CDCl_3$, 500 MHz): $\delta_H = 8.69$ (s, 2H), 7.94–7.96 (m, 2H), 7.47–7.51 (m, 2H), 7.33–7.37 (m, 5H), 5.12 (s, 2H); ^{13}C NMR ($CDCl_3$, 125 MHz): $\delta_C = 156.2$, 150.1, 149.1, 144.3, 135.5, 134.9, 131.2, 129.0, 128.7, 127.4, 124.3, 115.7, 108.2, 71.4; MS (ESI): $m/z = 307.10$ $[M+H]^+$.

4.1.13. 4-(4-Nitro-2-phenethoxyphenyl)pyridine (**8**)

The title compound was synthesized from 1-bromo-4-nitro-2-phenethoxybenzene **5a** (150 mg, 0.47 mmol) according to method C using 4-pyridylboronic acid. The crude product was purified by flash chromatography on silica gel using a mixture of petroleum ether/ethyl acetate (2:1) as eluent. Yield: 104 mg (70%); yellow solid: mp 112–114 °C; $R_f = 0.32$ (n-Hex/EtOAc 1:2); Anal. $C_{19}H_{16}N_2O_3$ (C, H, N, O). ^1H NMR ($CDCl_3$, 500 MHz): $\delta_H = 8.60$ (dd, $J = 1.6$, 4.5 Hz, 2H), 7.87 (dd, $J = 2.2$, 8.4 Hz, 1H), 7.79 (d, $J = 2.1$ Hz, 1H), 7.40 (d, $J = 8.4$ Hz, 1H), 7.25–7.29 (m, 2H), 7.22–7.24 (m, 3H), 7.12–7.14 (m, 2H), 4.31 (t, $J = 6.4$ Hz, 2H), 3.04 (t, $J = 6.5$ Hz, 2H); ^{13}C NMR ($CDCl_3$, 125 MHz): $\delta_C = 156.5$, 150.0, 149.1, 144.2, 137.8, 134.5, 131.0, 129.2, 128.8, 127.0, 124.3, 116.3, 107.3, 70.1, 35.6; MS (ESI): $m/z = 321.12$ $[M+H]^+$.

4.1.14. 4-(4-Nitro-2-(3-phenylpropoxy)phenyl)pyridine (**9**)

The title compound was synthesized from 1-bromo-4-nitro-2-phenethoxybenzene **6a** (150 mg, 0.45 mmol) according to method C using 4-pyridylboronic acid. The crude product was purified by flash chromatography on silica gel using a mixture of petroleum ether/ethyl acetate (2:1) as eluent. Yield: 113 mg (76%); yellow solid: mp 127–199 °C; $R_f = 0.32$ (n-Hex/EtOAc 1:2); Anal. $C_{20}H_{18}N_2O_3$ (C, H, N, O). ^1H NMR ($CDCl_3$, 500 MHz): $\delta_H = 8.71$ (s, br, 2H), 7.91 (s, br, 1H), 7.79 (s, 1H), 7.45–7.47 (m, 3H), 7.23–7.27 (m, 2H), 7.15–7.19 (m, 1H), 7.10–7.12 (m, 2H), 4.09 (t, $J = 6.2$ Hz, 2H), 2.71 (t, $J = 7.3$ Hz, 2H), 2.06–2.10 (m, 2H); ^{13}C NMR ($CDCl_3$, 125 MHz): δ_C = 156.3, 149.8, 148.9, 144.2, 140.7, 134.3, 130.8, 128.6, 128.3, 126.2, 124.0, 116.0, 107.2, 68.2, 32.1, 30.5; MS (ESI): *m*/*z* = 335.13 [M+H]$^+$.

*4.1.15. 3-(4-Nitro-3-phenethoxyphenyl)pyridine (**10**)*

The title compound was synthesized from 4-bromo-1-nitro-2-phenethoxybenzene **10a** (108 mg, 0.34 mmol) according to method D using 3-pyridylboronic acid. The crude product was purified by flash chromatography on silica gel using a mixture of petroleum ether/ethyl acetate (2:1) as eluent. Yield: 106 mg, (97%); orange solid: mp = 91–92 °C; R_f = 0.36 (n-Hex/EtOAc 1:2); Anal. $C_{19}H_{16}N_2O_3$ (C, H, N, O). IR (ATR): $\bar{\nu}$ (cm^{-1}) = 3040 (m), 2940 (m), 1586 (s), 1505 (s), 1228 (s), 1022 (s), 734 (vs), 694 (vs); ^{1}H NMR ($CDCl_3$, 500 MHz): δ_H = 8.78 (s, 1H), 8.63 (d, *J* = 4.7 Hz, 1H), 7.90 (d, *J* = 8.5 Hz, 1H), 7.88 (d, *J* = 7.3 Hz, 1H), 7.40–7.46 (m, 1H), 7.26–7.30 (m, 4H), 7.18–7.23 (m, 1H), 7.14 (dd, *J* = 1.4, 8.4 Hz, 1H), 7.11 (s, 1H), 4.32 (t, *J* = 6.8 Hz, 2H), 3.14 (t, *J* = 6.8 Hz, 2H); ^{13}C NMR ($CDCl_3$, 125 MHz); δ_C = 152.9, 148.5, 147.0, 143.3, 139.5, 137.4, 135.8, 135.4, 129.2, 128.6, 126.8, 126.5, 124.2, 119.1, 113.2, 70.9, 35.7; MS (ESI): *m*/*z* = 320.88 [M+H]$^+$.

*4.1.16. 4-(4-Nitro-3-phenethoxyphenyl)pyridine (**11**)*

The title compound was synthesized from 4-bromo-1-nitro-2-phenethoxybenzene **11a** (139 mg, 0.43 mmol) according to method D using 4-pyridylboronic acid. The crude product was purified by flash chromatography on silica gel using a mixture of petroleum ether/ethyl acetate (1:1) as eluent. Yield: 129 mg (94%); ochre solid: mp = 98 °C; R_f = 0.27 (n-Hex/EtOAc 1:2); Anal. $C_{19}H_{16}N_2O_3$ (C, H, N, O). IR (ATR): $\bar{\nu}$ (cm^{-1}) = 3032 (m), 2951 (m), 1586 (s), 1552 (s), 1509 (s), 1225 (s), 808 (vs), 755 (vs), 698 (vs); ^{1}H NMR ($CDCl_3$, 500 MHz): δ_H = 8.66 (d, *J* = 5.4 Hz, 2H), 7.89 (d, *J* = 8.5 Hz, 1H), 7.44 (d, *J* = 5.0 Hz, 2H), 7.25–7.30 (m, 4H), 7.17–7.22 (m, 2H), 7.15 (d, *J* = 1.6 Hz, 1H), 4.32 (t, *J* = 6.8 Hz, 2H), 3.14 (t, *J* = 6.8 Hz, 2H); ^{13}C NMR ($CDCl_3$, 125 MHz); δ_C = 152.7, 149.7, 147.2, 143.8, 140.0, 137.4, 129.2, 128.6, 126.9, 126.4, 122.0, 119.0, 113.2, 70.9, 35.6; MS (ESI): *m*/*z* = 320.96 [M+H]$^+$.

*4.1.17. 3-(4-Fluoro-2-phenethoxyphenyl)pyridine (**12**)*

The title compound was synthesized from 1-bromo-4-fluoro-2-phenethoxybenzene **12a** (118 mg, 0.40 mmol) according to method D using 3-pyridylboronic acid. The crude product was purified by flash chromatography on silica gel using a mixture of hexane/ethyl acetate (5:1) as eluent. Yield: 86 mg (73%); brown oil; R_f = 0.66 (n-Hex/EtOAc 1:2); Anal. $C_{19}H_{16}FNO$ (C, H, N, O). IR (ATR): $\bar{\nu}$ (cm^{-1}) = 3029 (m), 2935 (m), 1599 (s), 1279 (s), 1160 (vs), 699 (vs); ^{1}H NMR ($CDCl_3$, 500 MHz): δ_H = 8.73 (d, *J* = 1.9 Hz, 2H), 7.69 (d, *J* = 1.4 Hz, 1H), 7.21–7.34 (m, 5H), 7.15 (d, *J* = 7.2 Hz, 2H), 6.70–6.76 (m, 2H), 4.19 (t, *J* = 6.5 Hz), 3.03 (t, *J* = 6.5 Hz); ^{13}C NMR ($CDCl_3$, 125 MHz): δ_C = 162.9 (d, J_{CF} = 244.7 Hz), 156.7, 149.5, 147.8, 138.2, 136.6, 132.8, 131.4 (d, J_{CF} = 10.1 Hz), 136.9, 123.0, 117.5, 107.2 (d, J_{CF} = 21.1 Hz), 100.7 (d, J_{CF} = 26.6 Hz), 69.1, 34.6; MS (ESI): *m*/*z* = 293.87 [M+H]$^+$.

*4.1.18. 4-(4-Fluoro-2-phenethoxyphenyl)pyridine (**13**)*

The title compound was synthesized from 1-bromo-4-fluoro-2-phenethoxybenzene **12a** (128 mg, 0.43 mmol) according to method D using 4-pyridylboronic acid. The crude product was purified by flash chromatography on silica gel using a mixture of hexane/ethyl acetate (5:1) as eluent. Yield: 89 mg (71%); fawn oil; R_f = 0.54 (n-Hex/EtOAc 1:2); Anal. $C_{19}H_{16}FNO$ (C, H, N, O). IR (ATR): $\bar{\nu}$ (cm^{-1}) = 3029 (m), 2936 (m), 1599 (vs), 1407 (s), 1280 (vs), 1161 (vs), 832 (vs), 699 (vs); ^{1}H NMR ($CDCl_3$, 500 MHz): δ_H = 8.54 (dd, *J* = 4.7, 1.6 Hz, 2H), 7.21–7.31 (m, 6H), 7.14–7.18 (m, 2H), 6.67–6.75 (m, 2H), 4.20 (t, *J* = 6.5 Hz, 2H), 3.03 (t, *J* = 6.5 Hz, 2H); ^{13}C NMR ($CDCl_3$, 125 MHz) δ_C = 35.4, 69.4, 100.4 (d, J_{CF} = 25.7 Hz), 107.7 (d, J_{CF} = 22.0 Hz), 123.6 (d, J_{CF} = 3.7 Hz), 124.4, 126.7, 128.5, 129.0, 131.3 (d, J_{CF} = 10.1 Hz), 137.8, 146.0, 148.8, 157.0 (d, J_{CF} = 9.2 Hz), 163.9 (d, J_{CF} = 248.4 Hz); MS (ESI): *m*/*z* = 293.91 [M+H]$^+$.

*4.1.19. 3-(4-Methoxy-2-phenethoxyphenyl)pyridine (**14**)*

The title compound was synthesized from 1-bromo-4-methoxy-2-phenethoxybenzene **14a** (100 mg, 0.33 mmol) according to method C using 3-pyridylboronic acid. The crude product was purified by flash chromatography on silica gel using a mixture of petroleum ether/ethyl acetate (2:1) as eluent. Yield: 78 mg (77%); lemon yellow oil; R_f = 0.55 (n-Hex/EtOAc 1:2); Anal. $C_{20}H_{19}NO_2$ (C, H, N, O). IR (ATR): $\bar{\nu}$ (cm^{-1}) = 3028 (m), 2934 (m), 2836 (m), 1883 (w), 1608 (s), 1165 (vs), 699 (vs); ^{1}H NMR ($CDCl_3$, 500 MHz): δ_H = 8.72 (d, *J* = 1.9 Hz, 1H), 8.55 (dd, *J* = 1.6, 4.7 Hz, 1H), 7.71–7.75 (m, 1H), 7.24–7.35 (m, 5H), 7.19–7.22 (m, 2H), 6.62 (dd, *J* = 2.2, 8.4 Hz, 1H), 6.58 (d, *J* = 2.2 Hz, 1H), 4.23 (t, *J* = 6.6 Hz, 2H), 3.87 (s, 3H), 3.07 (t, *J* = 6.6 Hz, 2H); ^{13}C NMR ($CDCl_3$, 125 MHz): δ_C = 161.0, 156.9, 149.5, 146.7, 138.1, 137.4, 134.3, 131.1, 129.0, 128.4, 126.5, 122.8, 119.8, 105.3, 99.8, 69.2, 55.4, 35.6; MS (ESI): *m*/*z* = 305.85 [M+H]$^+$.

*4.1.20. 4-(4-Methoxy-2-phenethoxyphenyl)pyridine (**15**)*

The title compound was synthesized from 1-bromo-4-methoxy-2-phenethoxybenzene **14a** (106 mg, 0.35 mmol) according to method C using 4-pyridylboronic acid. The crude product was purified by flash chromatography on silica gel using a mixture of petroleum ether/ethyl acetate (1:1) as eluent. Yield: 76 mg (71%); lemon yellow solid: mp 63–64 °C; R_f = 0.40 (n-Hex/EtOAc 1:2); Anal. $C_{20}H_{19}NO_2$ (C, H, N, O). IR (ATR): $\bar{\nu}$ (cm^{-1}) = 3028 (m), 2955 (m), 2835 (m), 1941 (w), 1610 (s), 1207 (vs), 696 (vs), 783 (vs); ^{1}H NMR ($CDCl_3$, 500 MHz): δ_H = 8.47 (dd, *J* = 1.6, 4.7 Hz, 2H), 7.17–7.28 (m, 6H), 7.13–7.17 (m, 2H), 6.53 (dd, *J* = 2.5, 8.5 Hz, 1H), 6.49 (d, *J* = 2.5 Hz, 1H), 4.17 (t, *J* = 6.5 Hz, 2H), 3.79 (s, 3H), 3.00 (t, *J* = 6.5 Hz, 2H); ^{13}C NMR ($CDCl_3$, 125 MHz): δ_C = 161.5, 157.0, 148.8, 146.5, 138.1, 131.1, 129.0, 128.5, 126.6, 124.2, 120.4, 105.4, 99.8, 69.1, 55.4, 35.6; MS (ESI): *m*/*z* = 305.86 [M+H]$^+$.

*4.1.21. 3-(2-Phenethoxy-4-(trifluoromethyl)phenyl)pyridine (**16**)*

The title compound was synthesized from 1-bromo-2-phenethoxy-4-(trifluoromethyl)benzene **16a** (106 mg, 0.31 mmol) according to method C using 3-pyridylboronic acid. The crude product was purified by flash chromatography on silica gel using a mixture of hexane/ethyl acetate (2:1) as eluent. Yield: 75 mg (70%); light yellow solid: mp = 43–44 °C; R_f = 0.68 (n-Hex/EtOAc 1:2); Anal. $C_{20}H_{16}F_3NO$ (C, H, N, O). IR (ATR): $\bar{\nu}$ (cm^{-1}) = 3031 (m), 2949 (m), 1614 (m), 1406 (s), 1328 (vs), 1105 (vs) 698 (vs); ^{1}H NMR ($CDCl_3$, 500 MHz): δ_H = 8.68 (dd, *J* = 0.8, 2.4 Hz, 1H), 8.60 (dd, *J* = 1.6, 4.7 Hz, 1H), 7.66–7.69 (m, 1H), 7.37–7.40 (m, 1H), 7.20–7.31 (m, 5H), 7.15–7.17 (m, 1H), 7.12–7.15 (m, 2H), 4.24 (t, *J* = 6.6 Hz, 2H), 3.03 (t, *J* = 6.6 Hz, 2H); ^{13}C NMR ($CDCl_3$, 125 MHz): δ_C = 156.0, 149.8, 148.4, 137.8, 137.2, 133.0, 131.5 (q, J_{CF} = 32.5 Hz), 130.9, 130.6, 129.0, 128.5, 126.6, 122.9, 123.8 (q, J_{CF} = 272.2 Hz), 117.8 (q, J_{CF} = 3.7 Hz), 108.8 (q, J_{CF} = 3.7 Hz), 69.5, 35.5; MS (ESI): *m*/*z* = 343.81 [M+H]$^+$.

*4.1.22. 4-(2-Phenethoxy-4-(trifluoromethyl)phenyl)pyridine (**17**)*

The title compound was synthesized from 1-bromo-2-phenethoxy-4-(trifluoromethyl)benzene **16a** (100 mg, 0.29) according to method C using 4-pyridylboronic acid. The crude product was purified by flash chromatography on silica gel using a mixture of petroleum ether/ethyl acetate (4:1) as eluent. Yield: 73 mg (73%); light fawn solid: mp = 58–59 °C; R_f = 0.55 (n-Hex/EtOAc 1:2); Anal. $C_{20}H_{16}F_3NO$ (C, H, N, O). IR (ATR): $\bar{\nu}$ (cm^{-1}) = 3033 (m), 2946 (m), 1591 (s), 1329 (vs), 1109 (vs), 817 (vs); ^{1}H NMR ($CDCl_3$, 500 MHz): δ_H = 8.57 (dd, *J* = 1.6, 4.4 Hz, 2H), 7.37 (dd, *J* = 7.9, 0.6 Hz, 1H), 7.24–7.29 (m, 5H), 7.20–7.24 (m, 1H), 7.12–7.17 (m, 3H), 4.25 (t, *J* = 6.3 Hz, 2H), 3.02 (t, *J* = 6.3 Hz, 2H); ^{13}C NMR ($CDCl_3$, 125 MHz): δ_C = 155.9, 149.2, 145.2, 137.8, 132.1 (q, J_{CF} = 33.0 Hz), 131.1, 130.8, 129.0, 128.5, 126.7, 124.3, 123.7 (q, J_{CF} = 272.2 Hz), 117.8 (q, J_{CF} = 3.7 Hz), 108.9 (q, J_{CF} = 3.7 Hz), 69.5, 35.5; MS (ESI): *m/z* = 343.82 [M+H]$^+$.

*4.1.23. 3-Phenethoxy-4-(pyridin-3-yl)benzonitrile (**18**)*

The title compound was synthesized from 4-bromo-3-phenethoxybenzonitrile **18a** (105 mg, 0.35 mmol) according to method D using 3-pyridylboronic acid. The crude product was purified by flash chromatography on silica gel using a mixture of petroleum ether/ethyl acetate (1.5:1) as eluent. Yield: 82 mg, (78%); brown oil; R_f = 0.56 (n-Hex/EtOAc 1:2); Anal. $C_{20}H_{16}N_2O$ (C, H, N, O). IR (ATR): $\bar{\nu}$ (cm^{-1}) = 3029 (m), 2936 (m), 2228 (s), 1506 (s), 1397 (s), 1277 (vs), 1021 (s), 700 (vs); ^{1}H NMR ($CDCl_3$, 500 MHz): δ_H = 8.7 (br, s, 1H) 8.6 (br, s, 1H) 7.7 (d, *J* = 7.6 Hz, 1H) 7.3–7.4 (m, 3H) 7.2–7.3 (m, 4H) 7.1–7.2 (m, 2H) 4.3 (t, *J* = 6.5 Hz, 2H) 3.1 (t, *J* = 6.5 Hz, 2H); ^{13}C NMR ($CDCl_3$, 125 MHz): δ_C = 156.0, 149.2, 148.2, 137.5, 134.4, 132.8, 131.8, 131.2, 128.9, 128.5, 126.7, 125.0, 123.1, 118.4, 115.1, 113.0, 69.6, 35.4; MS (ESI): *m/z* = 300.96 [M+H]$^+$.

*4.1.24. 3-Phenethoxy-4-(pyridin-4-yl)benzonitrile (**19**)*

The title compound was synthesized from 4-bromo-3-phenethoxybenzonitrile **18a** (110 mg, 0.36 mmol) according to method D using 4-pyridylboronic acid. The crude product was purified by flash chromatography on silica gel using a mixture of petroleum ether/ethyl acetate (1.5:1) as eluent. Yield: 92 mg, (85%); white solid: mp = 112–113 °C; R_f = 0.44 (n-Hex/EtOAc 1:2); Anal. $C_{20}H_{16}N_2O$ (C, H, N, O). IR (ATR): $\bar{\nu}$ (cm^{-1}) = 3031 (m), 2928 (m), 2228 (s), 1595 (s), 1277 (s), 1024 (s), 808 (vs), 752 (vs), 705 (vs); ^{1}H NMR ($CDCl_3$, 500 MHz): δ_H = 8.6 (d, *J* = 6.0 Hz, 2H), 7.4 (d, *J* = 7.9 Hz, 1H), 7.3 (dd, *J* = 1.6, 7.6 Hz, 1H), 7.2–7.3 (m, 5H), 7.2 (d, *J* = 1.6 Hz, 1H) 7.1–7.2 (m, 2H), 4.3 (t, *J* = 6.5 Hz, 2H), 3.1 (t, *J* = 6.5 Hz, 2H); ^{13}C NMR ($CDCl_3$, 125 MHz): δ_C = 155.9, 149.4, 144.5, 137.6, 132.6, 131.1, 128.9, 128.5, 126.8, 124.9, 124.1, 118.4, 115.2, 113.4, 69.6, 35.4; MS (ESI): *m/z* = 300.96 [M+H]$^+$.

*4.1.25. N,N-dimethyl-3-phenethoxy-4-(pyridin-3-yl)benzamide (**20**)*

The title compound was synthesized from 4-bromo-*N,N*-dimethyl-3-phenethoxybenzamide **20a** (100 mg, 0.29 mmol) according to method C using 3-pyridylboronic acid. The crude product was purified by flash chromatography on silica gel using ethyl acetate as eluent. Yield: 95 mg (95%); fawn solid: mp = 161–162 °C; R_f = 0.05 (n-Hex/EtOAc 1:2); Anal. $C_{22}H_{22}N_2O_2$ (C, H, N, O). IR (ATR): $\bar{\nu}$ (cm^{-1}) = 3451 (br, m), 2927 (m), 1711 (m), 1609 (s), 1406 (s), 1329 (vs), 703 (s); ^{1}H NMR ($(CD_3)_2CO$, 500 MHz): δ_H = 8.69 (dd, *J* = 1.0, 2.2 Hz, 1H), 8.54 (dd, *J* = 1.6, 4.7 Hz, 1H), 7.78 (ddd, *J* = 1.9, 3.5, 7.9 Hz, 1H), 7.40 (d, *J* = 7.9 Hz, 1H), 7.36 (ddd, *J* = 0.8, 4.9, 7.9 Hz, 1H), 7.16 (d, *J* = 1.6 Hz, 1H), 7.09 (dd, *J* = 1.4, 7.7 Hz, 1H), 4.33 (t, *J* = 6.5 Hz, 2H), 3.02–3.07 (m, 8H); ^{13}C NMR ($(CD_3)_2CO$, 125 MHz): δ_C = 171.1, 156.8, 150.9, 149.1, 139.6, 138.7, 137.7, 134.4, 131.1, 130.1, 129.2, 129.0, 127.2, 123.8, 120.6, 112.4, 70.2, 60.6, 36.3; MS (ESI): *m/z* = 346.81 [M+H]$^+$.

*4.1.26. N,N-dimethyl-3-phenethoxy-4-(pyridin-4-yl)benzamide (**21**)*

The title compound was synthesized from 4-bromo-*N,N*-dimethyl-3-phenethoxybenzamide **20a** (96 mg, 0.28 mmol) according to method C using 4-pyridylboronic acid. The crude product was purified by flash chromatography on silica gel using ethyl acetate as eluent. Yield: 76 mg (78%); white solid: mp = 262–263 °C; R_f = 0.05 (n-Hex/EtOAc 1:2); Anal. $C_{22}H_{22}N_2O_2$ (C, H, N, O). IR (ATR): $\bar{\nu}$ (cm^{-1}) = 3438 (br, m), 2933 (m), 1609 (s), 1414 (s), 1315 (vs), 700 (s); ^{1}H NMR (DMSO-d_6, 500 MHz): δ_H = 8.53 (dd, *J* = 1.6, 4.5 Hz, 2H), 7.41 (d, *J* = 7.6 Hz, 1H), 7.35 (dd, *J* = 1.6, 4.5 Hz, 2H), 7.25–7.30 (m, 2H), 7.19–7.24 (m, 3H), 7.15 (d, *J* = 1.6 Hz, 1H), 7.05 (dd, *J* = 1.6, 7.6 Hz, 1H), 4.30 (t, *J* = 6.5 Hz, 2H), 2.85–3.05 (m, 8H); ^{13}C NMR (DMSO-d_6, 125 MHz): δ_C = 169.4, 155.3, 149.3, 144.8, 138.5, 138.4, 130.2, 129.0, 128.2, 127.4, 126.3, 124.0, 119.4, 111.3, 68.9, 34.8; MS (ESI): *m/z* = 346.80 [M+H]$^+$.

*4.1.27. 3-Phenethoxy-2,3′-bipyridine (**22**)*

The title compound was synthesized from 2-bromo-3-phenethoxypyridine **22a** (95 mg, 0.342 mmol) according to method C using 3-pyridylboronic acid. The crude product was purified by flash chromatography on silica gel using ethyl acetate as eluent. Yield: 92 mg, (97.5%); light yellow solid: mp = 126–127 °C; R_f = 0.14 (n-Hex/EtOAc 1:2); Anal. $C_{18}H_{16}N_2O$ (C, H, N, O). IR (ATR): $\bar{\nu}$ (cm^{-1}) = 3510 (br, m), 2990 (m), 1579 (m), 1452 (s), 1321 (vs), 696 (s); ^{1}H NMR ($CDCl_3$, 500 MHz): δ_H = 9.2 (dd, *J* = 0.6, 2.2 Hz, 1H), 8.6 (dd, *J* = 1.6, 5.0 Hz, 1H), 8.3 (dd, *J* = 1.4, 4.6 Hz, 1H), 8.2 (dt, *J* = 2.0, 8.0 Hz, 1H), 7.4 (ddd, *J* = 0.8, 4.8, 8.0 Hz, 1H), 7.3–7.3 (m, 3H), 7.2–7.3 (m, 4H), 4.3 (t, *J* = 6.6 Hz, 2H), 3.1 (t, *J* = 6.6 Hz, 2H); ^{13}C NMR ($CDCl_3$, 125 MHz): δ_C = 153.2, 149.8, 148.2, 144.7, 141.8, 137.6, 137.4, 133.7, 129.0, 128.6, 126.8, 123.8, 123.0, 119.5, 69.4, 35.6; MS (ESI): *m/z* = 276.95 [M+H]$^+$.

*4.1.28. 3-Phenethoxy-2,4′-bipyridine (**23**)*

The title compound was synthesized from 2-bromo-3-phenethoxypyridine **22a** (50 mg, 0.18 mmol) according to method D using 4-pyridylboronic acid. The crude product was purified by flash chromatography on silica gel using ethyl acetate as eluent. Yield: 35 mg, (70.4%); light brown solid: mp = 39–40 °C; R_f = 0.16 (n-Hex/EtOAc 1:2); Anal. $C_{18}H_{16}N_2O$ (C, H, N, O). IR (ATR): $\bar{\nu}$ (cm^{-1}) = 3454 (br, m), 1642 (m), 1437 (s), 1322 (vs), 1272 (s), 814 (s), 744 (s), 699 (s); ^{1}H NMR ($CDCl_3$, 500 MHz): δ_H = 8.6 (d, *J* = 4.7 Hz, 2H), 8.3 (dd, *J* = 1.6, 4.4 Hz, 1H), 7.7 (d, *J* = 5.4 Hz, 2H), 7.2–7.3 (m, 7H), 4.3 (t, *J* = 6.6 Hz, 2H), 3.1 (t, *J* = 6.6 Hz, 2H); ^{13}C NMR ($CDCl_3$, 125 MHz): δ_C = 153.7, 149.6, 145.3, 145.1, 141.9, 137.9, 129.2, 128.8, 127.0, 124.6, 124.0, 119.9, 69.5, 35.8; MS (ESI): *m/z* = 276.97 [M+H]$^+$.

*4.1.29. 3-(4-Nitro-2-phenethoxybenzyl)pyridine (**24**)*

The title compound was synthesized from 4,4,5,5-tetramethyl-2-(4-nitro-2-phenethoxyphenyl)-1,3,2-dioxaborolane **24a** (97 mg, 0.26 mmol) according to method D using 3-pyridylboronic acid. The crude product was purified by flash chromatography on silica gel using a mixture of hexane/ethyl acetate (2:1) as eluent. Yield: 55 mg (63%); light brown solid: mp = 82–83 °C; R_f = 0.48 (n-Hex/EtOAc 1:2); Anal. $C_{20}H_{18}N_2O_3$ (C, H, N, O). IR (ATR): $\bar{\nu}$ (cm^{-1}) = 3061 (m), 2928 (m), 2879 (m), 1585 (m), 1511 (vs), 1337 (vs), 1248 (vs), 1026 (s), 744 (vs), 704 (vs); ^{1}H NMR ($CDCl_3$, 500 MHz): δ_H = 8.48 (br, s, 2H), 7.78 (dd, *J* = 8.2, 2.2 Hz, 1H), 7.70 (d, *J* = 2.2 Hz, 1H), 7.38 (d, *J* = 7.9 Hz, 1H), 7.30–7.35 (m, 2H), 7.24–7.28 (m, 3H), 7.22 (d, *J* = 8.2 Hz, 1H), 7.18 (dd, *J* = 7.4, 4.9 Hz, 1H), 4.30 (t, *J* = 6.6 Hz, 2H), 3.95 (s, 2H), 3.13 (t, *J* = 6.6 Hz, 2H); ^{13}C NMR ($CDCl_3$, 125 MHz) δ_C = 156.6, 149.8, 147.8, 147.4, 137.6, 136.5, 136.0, 134.9, 130.3, 128.8, 128.6, 126.7, 123.5, 115.9, 106.2, 69.3, 35.5, 33.4; MS (ESI): *m/z* = 335.03 [M+H]$^+$.

*4.1.30. 4-(4-Nitro-2-phenethoxybenzyl)pyridine (**25**)*

The title compound was synthesized from 4,4,5,5-tetramethyl-2-(4-nitro-2-phenethoxyphenyl)-1,3,2-dioxaborolane **24a** (80 mg, 0.22 mmol) according to method D using 4-pyridylboronic acid. The crude product was purified by flash chromatography on silica gel using a mixture of hexane/ethyl acetate (2:1) as eluent. Yield: 51 mg (69%); brown oil; Anal. C20H18N2O3 (C, H, N, O). R_f = 0.35 (n-Hex/EtOAc 1:2); IR (ATR): $\bar{\nu}$ (cm^{-1}) = 3028 (m), 2923 (m), 2851 (m), 1598 (m), 1517 (vs), 1341 (vs), 1247 (vs), 801 (s), 738 (vs), 700 (vs); ^{1}H NMR ($CDCl_3$, 500 MHz): δ_H = 8.45 (d, *J* = 6.0 Hz, 2H), 7.82 (dd, *J* = 8.2, 2.2 Hz, 1H), 7.74 (d, *J* = 2.2 Hz, 1H), 7.25–7.33 (m, 5H), 7.21 (dd, J = 7.7, 1.7 Hz, 2H), 7.10 (d, J = 6.3 Hz, 2H), 4.32 (t, J = 6.5 Hz, 2H), 4.02 (s, 2H), 3.10 (t, J = 6.5 Hz, 2H); ^{13}C NMR ($CDCl_3$, 125 MHz): δ_C = 156.7, 152.5, 148.2, 147.0, 140.7, 137.5, 134.1, 130.8, 128.7, 126.9, 124.7, 116.1, 106.4, 69.2, 35.9, 35.4; MS (ESI): m/z = 334.99 $[M+H]^+$.

4.2. Biology

4.2.1. Inhibition of hCYP11B1, hCYP11B2 and rCYP11B1

V79MZ*h*CYP11B1, V79MZ*h*CYP11B2 or V79MZ*r*CYP11B1 cells were pre-incubated with inhibitor for 1 h at 37 °C. The reaction was started by addition of 100 nM (*h*CYP11B) or 500 nM (*r*CYP11B1) [^{3}H]-11-deoxycorticosterone as substrate. After incubation for 25 min (*h*CYP11B1), 45 min (*h*CYP11B2) or 7 h (*r*CYP11B1), the enzyme reactions were stopped by extracting the supernatant with ethyl acetate. Samples were centrifuged, and the ethyl acetate was separated [46,50]. The steroids were separated by HPLC and analyzed with radio flow detection.

4.2.2. Inhibition of hCYP19

The inhibition of *h*CYP19 was determined in vitro using human placental microsomes with [1β-^{3}H]androstenedione as substrate [48].

4.2.3. Inhibition of hCYP17

Human CYP17 was expressed in *E. coli* (coexpressing human CYP17 and NADPH-P450 reductase) and the assay was performed as previously described [49].

4.3. Modeling studies

4.3.1. Establishment of hCYP11B1 homology model

The primary sequence of CYP11B1 *Homo sapiens* (UniProt code: P15538) was obtained from the Universal Protein Resource (UniProt, http://www.uniprot.org/), which was subsequently subject to similarity search in the UniProtKB database using the Basic Local Alignment Search Tool (BLAST) sever in UniProt. Among the hits, *h*CYP11B2 (UniProt code: P19099) with a crystal in complex with deoxycorticosterone (PDB ID: 4DVQ, chain A) that showed 93.2% identity and an E-value of 0.0 was selected as the template. The target and template proteins subsequently underwent a tree-based initial sequence alignment and then structural realignment taking into consideration the coordinates of alpha carbons in the *h*CYP11B2 crystal using MOE. After setting the force field to Amber99 with Solvation R Field, a library of ten initial models was generated employing the Generalized Born/Volume Integral (GB/VI) scoring function, from which the best one was selected according to electrostatic solvation energy and root mean square deviation of each intermediate model to the average position of all models.

4.3.2. Molecular dynamic simulation

The force field of Amber99 was firstly applied to the preliminary model, and the model was partially charged and energy-minimized to RMS Gradient of 0.1 before the initiation of molecular dynamic simulation using MOE. Conformations were generated in the statistical ensemble with thermodynamic variables of volume, temperature and number of particles being held as constants. The method of the Nosé–Poincaré–Anderson equations of motion was employed to create ensemble trajectory. The system was heated from 0 K to 300 K in 60 ps and, after a run time of 1 ns, it was cooled down to 0 K in 60 ps.

4.3.3. Molecular docking

The homology model was prepared by adding hydrogens and partial charges using the Protonate3D module in MOE. Compound **8** as the ligand was built and energy-minimized in the MMFF94s force field with MOE. After importing both the protein model and the ligand into GOLD, the heme iron was appointed as the origin of active-site with a radius 19 Å, although the function of automatic active-site detection was also switched on. A distance constraint of 1.5–4.5 Å between the heme iron and the coordinating N was set. Ligand was docked in 50 independent genetic algorithm iterations for each run with default parameters. The resulting binding poses were evaluated using the goldscore function with p450_pdb parameters and subsequently ranked according to fitness. The diverse binding modes were further investigated and illustrated with the LigX module in MOE.

Acknowledgments

We thank Jeannine Jung for performing the in vitro tests and are grateful to Prof. J. J. Rob Hermans, University of Maastricht, The Netherlands, for providing the V79MZ*h*CYP11B1 cells.

Appendix A. Supplementary data

Supplementary data related to this article can be found at http://dx.doi.org/10.1016/j.ejmech.2015.04.013.

References

[1] C. Steffensen, A.M. Bak, K.Z. Rubeck, J.O. Jørgensen, Epidemiology of Cushing's syndrome, Neuroendocrinology 92 (Suppl. 1) (2010) 1–5.
[2] R.N. Clayton, Mortality in Cushing's disease, Neuroendocrinology 92 (Suppl. 1) (2010) 71–76.
[3] D. Plotz, A.I. Knowlton, C. Ragan, The natural history of Cushing's disease, Am. J. Med. 13 (1952) 597–614.
[4] B. Catargi, V. Rigalleau, A. Poussin, N. Ronci-Chaix, V. Bex, V. Vergnot, H. Gin, P. Roger, A. Tabarin, Occult Cushing's syndrome in type-2 diabetes, J. Clin. Endocrinol. Metab. 88 (2003) 5808–5813.
[5] I. Chiodini, M.L. Mascia, S. Muscarella, C. Battista, S. Minisola, M. Arosio, S.A. Santini, G. Guglielmi, V. Carnevale, A. Scillitani, Subclinical hypercortisolism among outpatients referred for osteoporosis, Ann. Intern. Med. 147 (2007) 541–548.
[6] S. Guldiken, B. Guldiken, Subclinical Cushing's syndrome is a potential cause of metabolic dementia and rapidly progressive Alzheimer-type dementia, Med. Hypotheses 71 (2008) 703–705.
[7] E. Valassi, I. Crespo, I. Gich, J. Rodriguez, S.M. Webb, A reappraisal of the medical therapy with steroidogenesis inhibitors in Cushing's syndrome, Clin. Endocrinol. 77 (2012) 735–742.
[8] W.J. Jeffcoate, L.H. Rees, S. Tomlin, A.E. Jones, C.R.W. Edwards, G.M. Besser, Metyrapone in long-term management of Cushing's disease, Br. Med. J. 2 (1977) 215–217.
[9] M. Inagaki, N. Akizuki, A. Kugaya, H. Fujii, T. Akechi, Y. Uchitomi, Metyrapone for Cushing's syndrome, Am. J. Psychiatry 159 (2002), 1246–1246.
[10] X. Bertagna, R. Pivonello, M. Fleseriu, Y. Zhang, P. Robinson, A. Taylor, C.E. Watson, M. Maldonado, A.H. Hamrahian, M. Boscaro, B.M. Biller, LCI699, a potent 11β-hydroxylase inhibitor, normalizes urinary cortisol in patients with Cushing's disease: results from a multicenter, proof-of-concept study, J. Clin. Endocrinol. Metab. 99 (2014) 1375–1383.
[11] W. Zhu, Q. Hu, N. Hanke, C.J. van Koppen, R.W. Hartmann, Potent 11β-hydroxylase inhibitors with inverse metabolic stability in human plasma and hepatic S9 fractions to promote wound healing, J. Med. Chem. 57 (2014) 7811–7817.
[12] S. Guo, L.A. DiPietro, Factors affecting wound healing, J. Dent. Res. 89 (2010) 219–229.
[13] X.Y. Zhao, P.J. Malloy, A.V. Krishnan, S. Swami, N.M. Navone, D.M. Peehl, D. Feldman, Glucocorticoids can promote androgen-independent growth of prostate cancer cells through a mutated androgen receptor, Nat. Med. 6 (2000) 703–706.
[14] L. Yin, Q. Hu, R.W. Hartmann, Recent progress in pharmaceutical therapy for castration-resistant prostate cancer, Int. J. Mol. Sci. 14 (2013) 13958–13978.
[15] Q. Hu, C. Jagusch, U.E. Hille, J. Haupenthal, R.W. Hartmann, Replacement of imidazolyl by pyridyl in biphenyl methylenes results in selective CYP17 and dual CYP17/CYP11B1 inhibitors for the treatment of prostate cancer, J. Med. Chem. 53 (2010) 5749–5758.
[16] Q. Hu, L. Yin, R.W. Hartmann, Aldosterone synthase inhibitors as promising treatments for mineralocorticoid dependent cardiovascular and renal diseases, J. Med. Chem. 57 (2014) 5011–5022.
[17] L. Roumen, J.W. Peeters, J.M.A. Emmen, I.P.E. Beugels, E.M.G. Custers, M. de Gooyer, R. Plate, K. Pieterse, P.A.J. Hilbers, J.F.M. Smits, J.A.J. Vekemans, D. Leysen, H.C.J. Ottenheijm, H.M. Janssen, J.J.R. Hermans, Synthesis, biological

evaluation, and molecular modeling of 1-benzyl-1H-imidazoles as selective inhibitors of aldosterone synthase (CYP11B2), J. Med. Chem. 53 (2010) 1712–1725.
[18] E.L. Meredith, G. Ksander, L.G. Monovich, J.P. Papillon, Q. Liu, K. Miranda, P. Morris, C. Rao, R. Burgis, M. Capparelli, Q.Y. Hu, A. Singh, D.F. Rigel, A.Y. Jeng, M. Beil, F. Fu, C.W. Hu, D. LaSala, Discovery and in vivo evaluation of potent dual CYP11B2 (aldosterone synthase) and CYP11B1 inhibitors, ACS Med. Chem. Lett. 4 (2013) 1203–1207.
[19] Q. Hu, L. Yin, A. Ali, A.J. Cooke, J. Bennett, P. Ratcliffe, M.M. Lo, E. Metzger, S. Hoyt, R.W. Hartmann, Novel pyridyl substituted 4,5-dihydro-[1,2,4]triazolo [4,3-a]quinolines as potent and selective aldosterone synthase inhibitors with improved in vitro metabolic stability, J. Med. Chem. 58 (2015) 2530–2537.
[20] S. Lucas, M. Negri, R. Heim, C. Zimmer, R.W. Hartmann, Fine-tuning the selectivity of aldosterone synthase inhibitors: insights from studies from studies of heteroaryl substituted 1,2,5,6-tetrahydropyrrolo[3,2,1-*ij*]quinoline-4-one derivatives, J. Med. Chem. 54 (2011) 2307–2319.
[21] L. Yin, Q. Hu, J. Emmerich, M.M. Lo, E. Metzger, A. Ali, R.W. Hartmann, Novel pyridyl- or isoquinolinyl- substituted indolines and indoles as potent and selective aldosterone synthase inhibitors, J. Med. Chem. 57 (2014) 5179–5189.
[22] L. Yin, Q. Hu, R.W. Hartmann, 3-Pyridinyl substituted aliphatic cycles as CYP11B2 inhibitors: aromaticity abolishment of the core significantly increased selectivity over CYP1A2, PLoS One 7 (11) (2012) e48048, http://dx.doi.org/10.1371/journal.pone.0048048.
[23] S. Gobbi, Q. Hu, M. Negri, C. Zimmer, F. Belluti, A. Rampa, R.W. Hartmann, A. Bisi, Modulation of cytochromes P450 with xanthone-based molecules: from aromatase to aldosterone synthase and steroid 11β-hydroxylase inhibition, J. Med. Chem. 56 (2013) 1723–1729.
[24] C.M. Grombein, Q. Hu, R. Heim, S. Rau, C. Zimmer, R.W. Hartmann, 1-Phenylsulfinyl-3-(pyridin-3-yl)naphthalen-2-ols: a new class of potent and selective aldosterone synthase inhibitors, Eur. J. Med. Chem. 89 (2015) 597–605.
[25] C.M. Grombein, Q. Hu, S. Rau, C. Zimmer, R.W. Hartmann, Heteroatom insertion into 3,4-dihydro-1H-quinolin-2-ones leads to potent and selective inhibitors of human and rat aldosterone synthase, Eur. J. Med. Chem. 90 (2015) 788–796.
[26] M.A.E. Pinto-Bazurco Mendieta, Q. Hu, M. Engel, R.W. Hartmann, Highly potent and selective non-steroidal dual inhibitors of CYP17/CYP11B2 for the treatment of prostate cancer to reduce risks of cardiovascular diseases, J. Med. Chem. 56 (2013) 6101–6107.
[27] Q. Hu, M. Negri, S. Olgen, R.W. Hartmann, The role of fluorine substitution in biphenyl methylene imidazole type CYP17 inhibitors for the treatment of prostate carcinoma, ChemMedChem. 5 (2010) 899–910.
[28] Q. Hu, L. Yin, C. Jagusch, U.E. Hille, R.W. Hartmann, Isopropylidene substitution increases activity and selectivity of biphenyl methylene 4-pyridine type CYP17 inhibitors, J. Med. Chem. 53 (2010) 5049–5053.
[29] U.E. Hille, Q. Hu, C. Vock, M. Negri, M. Bartels, U. Mueller-Vieira, T. Lauterbach, R.W. Hartmann, Novel CYP17 inhibitors: synthesis, biological evaluation, structure-activity relationships and modeling of methoxy- and hydroxy-substituted methyleneimidazolyl biphenyls, Eur. J. Med. Chem. 44 (2009) 2765–2775.
[30] U.E. Hille, Q. Hu, M.A.E. Pinto-Bazurco Mendieta, M. Bartels, C.A. Vock, T. Lauterbach, R.W. Hartmann, Steroidogenic cytochrome P450 (CYP) enzymes as drug targets: combining substructures of known CYP inhibitors leads to compounds with different inhibitory profile, C. R. Chim. 12 (2009) 1117–1126.
[31] Q. Hu, M. Negri, K. Jahn-Hoffmann, Y. Zhuang, S. Olgen, M. Bartels, U. Müller-Vieira, T. Lauterbach, R.W. Hartmann, Synthesis, biological evaluation, and molecular modeling studies of methylene imidazole substituted biaryls as inhibitors of human 17α-hydroxylase-17,20-lyase (CYP17)-Part II: core rigidification and influence of substituents at the methylene bridge, Bioorg. Med. Chem. 16 (2008) 7715–7727.
[32] M.A.E. Pinto-Bazurco Mendieta, M. Negri, Q. Hu, U.E. Hille, C. Jagusch, K. Jahn-Hoffmann, U. Müller-Vieira, D. Schmidt, T. Lauterbach, R.W. Hartmann, CYP17 inhibitors. Annulations of additional rings in methylene imidazole substituted biphenyls: synthesis, biological evaluation and molecular modeling, Arch. Pharm. Weinh. 341 (2008) 597–609.
[33] C. Jagusch, M. Negri, U.E. Hille, Q. Hu, M. Bartels, K. Jahn-Hoffmann, M.A.E. Pinto-Bazurco Mendieta, B. Rodenwaldt, U. Müller-Vieira, D. Schmidt, T. Lauterbach, M. Recanatini, A. Cavalli, R.W. Hartmann, Synthesis, biological evaluation and molecular modeling studies of methyleneimidazole substituted biaryls as inhibitors of human 17α-hydroxylase-17,20-lyase (CYP17) – part I: heterocyclic modifications of the core structure, Bioorg. Med. Chem. 16 (2008) 1992–2010.
[34] A.H. Abadi, S.M. Abou-Seri, Q. Hu, M. Negri, R.W. Hartmann, Synthesis and biological evaluation of imidazolylmethylacridones as cytochrome P-450 enzymes inhibitors, MedChemComm. 3 (2012) 663–666.
[35] S. Gobbi, A. Cavalli, A. Rampa, F. Belluti, L. Piazzi, A. Paluszcak, R.W. Hartmann, M. Recanatini, A. Bisi, Lead optimization providing a series of flavone derivatives as potent nonsteroidal inhibitors of the cytochrome P450 aromatase enzyme, J. Med. Chem. 49 (2006) 4777–4780.
[36] M. Le Borgne, P. Marchand, M. Duflos, B. Delevoye-Seiller, S. Piessard-Robert, G. Le Baut, R.W. Hartmann, M. Palzer, Synthesis and in vitro evaluation of 3-(1-azolylmethyl)-1H-indoles and 3-(1-azoly1-1-phenylmethyl)-1H-indoles as inhibitors of P450 arom, Arch. Pharm. Weinh. Ger. 330 (1997) 141–145.
[37] M.P. Leze, M. Le Borgne, P. Pinson, A. Palusczak, M. Duflos, G. Le Baut, R.W. Hartmann, Synthesis and biological evaluation of 5-[(aryl)(1H-imidazol-1-yl)methyl]-1H-indoles: potent and selective aromatase inhibitors, Bioorg. Med. Chem. Lett. 16 (2006) 1134–1137.
[38] S. Gobbi, A. Cavalli, M. Negri, K.E. Schewe, F. Belluti, L. Piazzi, R.W. Hartmann, M. Recanatini, A. Bisi, Imidazolylmethylbenzophenones as highly potent aromatase inhibitors, J. Med. Chem. 50 (2007) 3420–3422.
[39] L. Yin, S. Lucas, F. Maurer, U. Kazmaier, Q. Hu, R.W. Hartmann, Novel imidazol-1-ylmethyl substituted 1,2,5,6-tetrahydro-pyrrolo[3,2,1-ij]quinolin-4-ones as potent and selective CYP11B1 inhibitors for the treatment of Cushing's syndrome, J. Med. Chem. 55 (2012) 6629–6633.
[40] J. Emmerich, Q. Hu, N. Hanke, R.W. Hartmann, Cushing's syndrome: development of highly potent and selective CYP11B1 inhibitors of the (pyridylmethyl)pyridine type, J. Med. Chem. 56 (2013) 6022–6032.
[41] U.E. Hille, C. Zimmer, J. Haupenthal, R.W. Hartmann, Optimization of the first selective steroid-11β-hydroxylase (CYP11B1) inhibitors for the treatment of cortisol dependent diseases, ACS Med. Chem. Lett. 2 (2011) 559–564.
[42] Q. Hu, L. Yin, R.W. Hartmann, Selective dual inhibitors of CYP19 and CYP11B2: targeting cardiovascular diseases hiding in the shadow of breast cancer, J. Med. Chem. 55 (2012) 7080–7089.
[43] L. Yin, Q. Hu, R.W. Hartmann, Tetrahydropyrroloquinolinone type dual inhibitors of aromatase/aldosterone synthase as a novel strategy for breast cancer patients with elevated cardiovascular risks, J. Med. Chem. 56 (2013) 460–470.
[44] S. Lucas, R. Heim, C. Ries, K.E. Schewe, B. Birk, R.W. Hartmann, In vivo active aldosterone synthase inhibitors with improved selectivity: lead optimization providing a series of pyridine substituted 3,4-dihydro-1H-quinolin-2-one derivatives, J. Med. Chem. 51 (2008) 8077–8087.
[45] U.E. Hille, C. Zimmer, C.A. Vock, R.W. Hartmann, Discovery of the first selective steroid-11β-hydroxylase (CYP11B1) inhibitors for the treatment of cortisol dependent diseases, ACS Med. Chem. Lett. 2 (2011) 2–6.
[46] P.B. Ehmer, M. Bureik, R. Bernhardt, U. Müller, R.W. Hartmann, Development of a test system for inhibitors of human aldosterone synthase (CYP11B2): screening in fission yeast and evaluation of selectivity in V79 cells, J. Steroid Biochem. Mol. Biol. 81 (2002) 173–179.
[47] G.F. Smith, Designing drugs to avoid toxicity, in: G. Lawton, D.R. Witty (Eds.), Progress in Medicinal Chemistry vol. 50, Elsevier Science, London, 2011, pp. 1–47.
[48] R.W. Hartmann, C. Batzl, Aromatase inhibitors. Synthesis and evaluation of mammary tumor inhibiting activity of 3-alkylated 3-(4-aminophenyl)piperidine-2,6-diones, J. Med. Chem. 29 (1986) 1362–1369.
[49] P.B. Ehmer, J. Jose, R.W. Hartmann, Development of a simple and rapid assay for the evaluation of inhibitors of human 17alpha-hydroxylase-C(17,20)-lyase (P450cl7) by coexpression of P450cl7 with NADPH-cytochrome-P450-reductase in Escherichia coli, J. Steroid Biochem. Mol. Biol. 75 (2000) 57–63.
[50] C. Ries, S. Lucas, R. Heim, B. Birk, R.W. Hartmann, Selective aldosterone synthase inhibitors reduce aldosterone formation in vitro and in vivo, J. Steroid Biochem. Mol. Biol. 116 (2009) 121–126.